ISTANBUL TECHNICAL UNIVERSITY ★ INFORMATICS INSTITUTE

QUASI-NEWTON AND ARTIFICIAL COMPRESSIBILITY BASED PARTITIONED ALGORITHMS FOR STRONGLY COUPLED FLUID STRUCTURE INTERACTIONS

M.Sc. THESIS

İbrahim ÖZKÜÇÜK

Computational Science and Engineering Department

Computational Science and Engineering Master Programme

JUNE 2017

ISTANBUL TECHNICAL UNIVERSITY ★ INFORMATICS INSTITUTE

**QUASI-NEWTON AND ARTIFICIAL COMPRESSIBILITY BASED
PARTITIONED ALGORITHMS FOR STRONGLY COUPLED
FLUID STRUCTURE INTERACTIONS**

M.Sc. THESIS

İbrahim ÖZKÜÇÜK
(702121022)

Computational Science and Engineering Department

Computational Science and Engineering Master Programme

Thesis Advisor: Prof. Dr. M. Serdar ÇELEBİ

JUNE 2017

İSTANBUL TEKNİK ÜNİVERSİTESİ ★ BİLİŞİM ENSTİTÜSÜ

SIKI BAĞLANMIŞ AKIŞKAN-KATI ETKİLEŞİMLİ PROBLEMLERDE QUASI-NEWTON VE YAPAY SIKIŞTIRILABİLME TABANLI BÖLÜMLENMİŞ ALGORİTMALAR

YÜKSEK LİSANS TEZİ

İbrahim ÖZKÜÇÜK
(702121022)

Hesaplamalı Bilim ve Mühendislik Anabilim Dalı

Hesaplamalı Bilim ve Mühendislik Yüksek Lisans Programı

Tez Danışmanı: Prof. Dr. M. Serdar ÇELEBİ

HAZİRAN 2017

İbrahim ÖZKÜÇÜK, a M.Sc. student of ITU Informatics InstituteEngineering and Technology 702121022 successfully defended the thesis entitled "QUASI-NEWTON AND ARTIFICIAL COMPRESSIBILITY BASED PARTITIONED ALGORITHMS FOR STRONGLY COUPLED FLUID STRUCTURE INTERACTIONS", which he/she prepared after fulfilling the requirements specified in the associated legislations, before the jury whose signatures are below.

Thesis Advisor :   **Prof. Dr. M. Serdar ÇELEBİ**   ....
Istanbul Technical University

Jury Members :   **Prof. Dr. M. Serdar ÇELEBİ**   ....
Istanbul Technical University

         Prof. Dr. Hakan AKYILDIZ   ....
Istanbul Technical University

         Assoc. Prof. Dr. Mine ÇAĞLAR   ....
Koç University

Date of Submission :   **5 May 2017**
Date of Defense :   **13 June 2017**

To my family,

TABLE OF CONTENTS

ABBREVIATIONS

1D	**:**	One dimensional
2D	**:**	Two dimensional
3D	**:**	Three dimensional
ALE	**:**	Arbitrary Lagrangian-Eularian
AC	**:**	Artificial compressibility
DN	**:**	Dirichlet-Neumann
DOF	**:**	Degrees of freedom
FDM	**:**	Finite difference method
FEM	**:**	Finite element method
FVM	**:**	Finite volume method
FSI	**:**	Fluid structure interactions
IAC	**:**	Interface artificial compressibility
IQN	**:**	Interface quasi-Newton
LS	**:**	Least squares
ND	**:**	Neumann-Dirichlet
NS	**:**	Navier-Stokes
RBF	**:**	Radial basis functions
QN	**:**	Quasi-Newton
WR	**:**	Weighted residuals

SYMBOLS

α	**:**	Womersley number
β	**:**	Artificial compressibility coefficient
γ	**:**	Displacement diffusion coefficient
$\Gamma_{F/S}$	**:**	Interface boundary between fluid and structure domains
ε	**:**	Error tolerance
μ	**:**	Viscosity
ν	**:**	Kinematic viscosity
ρ	**:**	Density
σ	**:**	Stress tensor
τ	**:**	Shear stress tensor
ω	**:**	Fundamental frequency
Ω_f	**:**	Fluid domain
Ω_s	**:**	Structure domain
b_f	**:**	Body forces acting on fluid
$\mathbf{d}$	**:**	Displacement vector
$\mathbf{D}$	**:**	The rate of deformation tensor
$\mathbf{I}$	**:**	Identity matrix
$\mathbf{J}$	**:**	Jacobian matrix
k	**:**	Iteration counter
L	**:**	Length
$\mathbf{n}$	**:**	Unit normal outward pointing vector
p	**:**	Pressure
r	**:**	Radius
$\mathbf{r}$	**:**	Residual vector
t	**:**	Time
$\mathbf{t}$	**:**	Traction field
$\mathbf{u}$	**:**	Fluid velocity field
$\mathbf{u_m}$	**:**	ALE coordinate system velocity
$\mathbf{x}$	**:**	Spatial coordinates

LIST OF TABLES

LIST OF FIGURES

QUASI-NEWTON AND ARTIFICIAL COMPRESSIBILITY BASED PARTITIONED ALGORITHMS FOR STRONGLY COUPLED FLUID STRUCTURE INTERACTIONS

SUMMARY

In this thesis, fluid-structure interactions (FSI), a multi-physics application, was investigated in detail. The reasons why fluid-structure interaction applications were developed, what those applications are, and different approaches that had been used on those FSI problems were explained and discussed.

The two coupling approaches in fluid-structure interactions, which are monolithic coupling and partitioned coupling, were explained briefly. Then, so called "black-box" partitioned FSI coupling schemes were investigated. Two numerical schemes of black-box partitioned FSI coupling methods, explicit and implicit, were explained in detail, the algorithmic differences between them were pointed out. Two algorithms based on implicit partitioned FSI coupling scheme, Aitken's dynamic relaxation and the state of the art IQN-LS methods were explained in detail. The solvers which use those algorithms were used in order to run famous FSI benchmark case [1]. The performances of both implicit partitioned algorithms were compared by using the benchmark case and discussed in detail. The superior performance of IQN-LS method over Aitken's dynamic relaxation was confirmed as a result of this comparison. Nevertheless, one of the major problem of partitioned coupling methods, which was described as the "incompressibility dilemma" by [2] for fully-enclosed, incompressible problems, was explored. A potential solution to this problem which was modifying the fluid solver and the coupling algorithm in order to add "artificial compressibility" was discussed briefly.

Lastly, fluid-structure interaction applications in hemodynamics and blood flow simulations were introduced. The reasons why FSI techniques are required in order to simulate the blood flow through artery simulations in hemodynamics were explained briefly. Nevertheless, the challenges in modeling the blood flow and artery walls were described and the effects of their highly nonlinear nature on FSI applications were discussed. Finally, the state of the art implicit partitioned FSI coupling scheme, IQN-LS, based solver was used in order to simulate 3D blood flow through large artery. The simulation was composed of incompressible, Newtonian, laminar flow solver with pulsatile velocity profile and linear elastic structural solver. All setup parameters and the results of the simulation were discussed in detail. The suitability of IQN-LS algorithm for further hemodynamics FSI applications were discussed.

SIKI BAĞLANMIŞ AKIŞKAN-KATI ETKİLEŞİMLİ PROBLEMLERDE QUASI-NEWTON VE YAPAY SIKIŞTIRILABİLME TABANLI BÖLÜMLENMİŞ ALGORİTMALAR

ÖZET

Bu tezde, çoklu fizik uygulaması olan akışkan-katı etkileşimleri derinlemesine incelenmiştir. Üç ana hedef konulmuş ve o hedeflere nasıl ulaşıldığı açıklanmış, tartışılmıştır.

Bu hedeflerden ilki, akışkan-katı etkileşimli problemlerin neler oldukları, hangi mühendislik alanlarında kullanıldıkları ve akışkan-katı etkileşimli uygulamaların neden yapıldıklarının incelenmesidir. Ayrıca günümüze kadar kullanılmış ve halen kullanılmakta olan akışkan-katı etkileşimli metodları derinlemesine incelemek, herkes tarafından "benchmark" problemi olarak tanınan bir problemde incelenen metodları kullanmak ve bu metodlar arasındaki performans farklılıklarını göstermektir.

İkinci hedef ise, tamamen kapalı, silindir şeklindeki damar içerisinde kan akışı simülasyonların temel karakteristiklerini ve sayısal çözümlerindeki zorluklarını belirlemektir.

Bu tezdeki son hedef ise, birinci bölümde elde edilen bulguların ışığında, en iyi performasa sahip olan akışkan-katı etkileşimi metodununun, damar içerisindeki kan akışı problemlerindeki performansını ölçmek ve gelecekteki akışkan-katı etkileşimli kan akışı simulasyonları için ne kadar uygun bir metod olabileceğini saptamaktır.

Akışkan-katı etkileşimli uygulamalar kısaca şöyle açıklanabilir. Bir akışkan ile bir katının oluşturduğu bir problemde, akışkan ile katı arasındaki etkileşim bilim veya mühendislik çerçeveleri içerisinde gözardı edilemeyecek kadar güçlüyse (sıkıysa); akışkan-katı etkileşim tabanlı sayısal metodlar kullanılarak o problem çözülmelidir. Aksi takdirde problemi çözmek için kullanılan simülasyonların sonuçları gerçeklerden daha uzak olacaktır. Belirli bir hızın üzerine çıkmış bir otomobilin hava ile etkileşimi, bir uçak kanadı tasarımında kanadın üzerine binen yüklerin hesapları, rüzgar türbinü kanatlarının eğrilme oranları veya damarlar içerisinde akan kanın yarattığı etkiler gözardı edilemeyecek kadar birbirine sıkı bağlanmış problemlerdir.

Akışkan-katı etkileşimli problemlerde ve onların sayısal çözümlerinde dikkate alınması gereken iki temel unsur vardır. Bunlar akışkan problemi ve katı problemleri arasındaki etkileşim sınırlarında, dinamik devamlılığın ve kinematik devamlılığın sağlanmasıdır. Dinamik devamlılık, etkileşim sınırlarında hem akışkandan hem de katıdan gelecek olan stresler ile kuvvetlerin her zaman birbirine eşit olmasıdır. Kinematik devamlılık ise, etkileşim sınırlarında hem akışkanda hem de katıda oluşabilecek olan yer değiştirmelerin birbirlerine eşit olmaları esasıdır.

Akışkan-katı etkileşimli problemlerde uygulanan metodlar iki ana grup altında sınıflandırılıyor. Bunlardan biri monolitik yaklaşım, diğeri ise bölümlenmiş yaklaşımdır. Monolitik yaklaşımda; akış, katı ve etkileşim problemlerindeki alan değişkenlerinin tek bir bünye denklemi olarak yazılması ve o denklemin tüm

problem geometrisinde çözülmesidir. Bölümlenmiş yaklaşımlarda ise; akışkan, katı ve etkileşim problemleri birbirlerinden bağımsız olarak çözdürülür ve problemin sonucuna yakınsamaya çalışılır. Bu tezde, her iki tip yaklaşım türü de incelenmiş ve ne oldukları kısaca anlatılmıştır. Bölümlenmiş yaklaşımlı metodların içinde "black-box" olarak adlandırılan yaklaşım, akışkan-katı etkileşimli problemlerin akışkan ve katı kısımlarını birbirlerinden en bağımsız olacak şekilde tutan yaklaşım türüdür. Bu tezdeki çalışmanın ana hatlarını da, bu "black-box" yaklaşımlı metodlar oluşturuyor.

"Black-box" yaklaşımlarında, birbirinden bağımsız çalışan hem akışkan model denklemleri çözücüsü hem de katı model denklemleri çözücüsü ve son olarak da aralarındaki etkileşimi sağlayacak olan "bağlantı problemi" çözücüsü mevcuttur. Akışkan ve katı problemlerinden gelen verilerin, bu iki alan arasındaki dinamik ve kinematik sürekliliğe uymalarını sağlayan "bağlantı problemi" çözücüsü problem türüne göre farklı şekillerde olabiliyor. Bu farklı tür metodlar da kendi içerisinde "explicit" ve "implicit" olarak iki ayrı sınıfa ayrılıyorlar. Herhangi bir sayısal metodda da geçerli olduğu üzere "explicit" olarak sınıflandırılan "bağlantı problemi" çözücülerinde, dinamik ve kinematik süreklilik sınır koşullarına, çözümün ulaşıp ulaşmadığı kontrol edilmemektedir. Bu yüzden de belli şartlara sahip olan problemlerde verimli çalışabilmektelerdir. "Implicit" olarak sınıflandırılan "bağlantı problemi" çözücülerinde ise çözümün belirlenen koşullara ulaşıp, ulaşmadığı kontrol edilir ve çözümün sınır koşullarına ulaşması sağlanır. Bu kontrol mekanizması da "implicit" olan metodlarının becerilerini, kararlılıklarını arttırmış olup, çözmesi çok daha zor olan sıkı etkileşimli akışkan-katı problemlerinde iyi performans göstermelerini sağlamıştır.

Bu tezde "implicit" olarak sınıflandırılan "black-box" bölümlenmiş akışkan-katı etkileşimleri metodlarından "Aitken's dynamic relaxation" ve quasi-Newton tabanlı "IQN-LS" metodları detaylıca incelenmiştir. Literatürde yaygın olarak kullanılan bir "benchmark" probleminde de bu iki bağlantı tiplerinin karşılaştırılması yapılmıştır. Günümüzde "the state of art" olarak tanınan metod olan "IQN-LS" metodu da incelenmiş olup, uygulamalarıyla diğerlerinden da iyi sonuç verdiği ve bunu çok daha kararlı ve hızlı bir şekilde yapabildiği gösterilmiş, bu üstün performansının kaynağı kısaca açıklanmıştır. Bunlarla birlikte, bölümlenmiş algoritmalarda gözlemlenen büyük bir problem incelenmiş ve çözüm aranmıştır. "Sıkıştırılamazlık ikilemi" olarak anılan problemin neden ortaya çıktığı kısaca bahsedilmiş ve problemin çözümler üzerindeki kötü etkilerini azaltacak bir teknik araştırılmıştır. "Yapay sıkıştırılabilme" olarak isimlendirilmiş olan bu tekniğin, IQN-LS metodu için uygulanabilirliği sorgulanmış ve teknik zorlukları tartışılmıştır.

Son olarak, kan akışı modellemelerindeki akışkan-katı etkileşimleri tanıtılmıştır. Kan akışı modelleri matematiksel ve sayısal olarak çözülmeleri en zor olan problem türüdür. Kanın ve kanı çevreleyen damarların aslında yaşayan bir matabolizmaya sahip olmaları bu zorlukları çıkaran birkaç sebepten biridir. Kanın akışmazlığını modellemek zor olsa da, mevcut modellerin çoğu "nonlineer"lik göstermektedir. Bununla birlikte aynı "nonlineer"lik damar duvarlarının elastikliğinde de gözlenmektedir. Dolayısıyla zaten "nonlineer" denklemlerin çözümündeki zorluklar hem de akışkan-katı probleminden gelen "nonlineer"lik, kan akışı problemlerindeki akışkan-katı etkileşimleri uygulamalarını çözmeyi çok zorlaştırıyor. Damarlar içindeki kan akışının modellenmesindeki bu zorlukların nasıl aşılabileceği araştırılmıştır. Denemelerde kendini göstermiş olan IQN-LS tabanlı akışkan-katı etkileşimleri

çözücümüzü kullanarak geniş damarlarda kan akışı modellemesi ve simülasyonu yapılmıştır. Bu simulasyon üç boyutta koşturulmuştur. Akış problemi şıkıştırılmaz, Newtonian ve laminer olarak modellenmiş olup, zamana bağlı değişen hız profili eklenmiştir. Katı problemi ise lineer elastik olarak modellenmiş ve neden bizim problemimize uygun olmadığı tartışılmıştır. Simülasyona ait tüm parametreler ve simülasyonun sonuçları detaylıca açıklanmış ve tartışılmıştır.

1. INTRODUCTION

The perceivable nature can be categorized as inherently multi-scale and multi-physics problems. Although, scientists have discovered and developed a great amount of theories and laws in order to reach an understanding of nature in a better, quantitative way; most of the developed theories and laws have only worked in their own scopes and had always some phenomenons that escaped from their limited scopes.

To overcome the limitations of theories and laws, coupled systems have been developing in contemporary science and engineering projects. By designing a coupling between different physical domains or different scales, better approximations of engineering problems to the reality of nature have been achieved. One class of such multi-physics problems is called Fluid-Structure Interaction (FSI) which focuses on the problems where mutual dependence and response between fluid and structure becomes significant.

In FSI problems, the flow behavior depends on the shape of the structure and its motion, whereas the motion and the deformation of the structure depends on the fluid forces acting on the structure. For instance, interaction between a slow car and the air surrounding it can be neglected thus computational fluid dynamics (CFD) can be used for modeling; however after passing a certain speed, the effects of the aerodynamics becomes significant thus FSI must be used in order to capture more realistic approximation. Several other examples of FSI problems can be listed as the fluttering of aircraft wings [3], deflection of wind-turbine blades, blood flow and arterial dynamics [4], blood flow in cerebral aneurysms [5] and rocking motion of the ships. Since FSI plays an important role in contemporary engineering applications, predictive FSI methods which would help modeling these problems of interest are in high demand in the industry, science and many other contexts.

One of the field that has started using FSI techniques for the last decade is biomechanics field where blood flow through arteries are modeled and hemodynamics are investigated. The reason for increasing usage of FSI in hemodynamics is because,

due to viscoelastic nature of the blood vessels, assumptions of rigid wall structure of the vessels had given unrealistic results. Moreover, it was discovered that there is a significant interaction between blood vessels and the blood flow inside of them so that FSI techniques must be used in order to get more realistic approximations about hemodynamics. According to [6] research, the rigid wall assumption, without FSI, in computations consistently shows an overestimation of wall shear stress compared to the flexible wall by as much as 50%. Consequently, the people who work on blood flow and hemodynamics have started using FSI techniques in order to simulate blood flow in arteries.

The field of FSI has been slowly reaching its maturity in the sense that many of its properties and complexities are in general well understood as well as with emerging methods to overcome the challenges involved. The inherently nonlinear and time dependent nature of the FSI makes it very difficult to use analytical methods for solving these class of problems. Therefore computational FSI research has had significant advances in the last decade by forming both core FSI methods and special FSI methods targeting specific classes of problems (see for example [7]). Most of the computational methods developed on the last decade are robust, efficient and capable of accurately modeling complex 3D geometries at full spatial scales. There are essentially two main approaches to solving FSI problems. One of them is monolithic approach and the other one is partitioned approach. The monolithic approach solves all the governing equations, which comes from fluid domain, solid domain and coupling interface domain, in a single unified solver, typically by using some variant of Newton's method [8]. On the other hand, partitioned approach uses two separate field solvers for both fluid and solid domains, coupled along an interface. Partitioned schemes can be solved either explicitly or implicitly (by using sub-iterations) in order to satisfy coupling interface conditions.

One of the important research area in FSI problems is about the simulation of incompressible flows. A number of numerical challenges emerges in incompressible FSI, especially when densities of fluid and solid domain are of equal orders of magnitude or the geometrical aspect ratio of the problem is large as in the simulation of blood flow through arteries. In such problems, the numerical coupling at the interface are non-trivial and another problem referred "added-mass effect" emerges [9].

In order to obtain a stable and robust solution procedure for these strongly coupled problems, monolithic solvers were advised or even required [10]. Although monolithic approach has its own advantages, it is hard to justify enormous initial investment required in developing a monolithic solver. Moreover, there are stable, robust and optimized large number of fluid and solid solvers available. Therefore, partitioned schemes can be counted as a better solution if a monolithic solver is not absolutely required. Nevertheless, partitioned approach lets use of different numerical schemes and discretisations on the sub-domain problems as long as data transfer between fluid and solid domain is also designed accordingly.

In partitioned FSI solvers, both fluid and solid solvers have iterations in order to solve their own problem. In addition to that, coupling algorithm has iterations on its own and in coupling's iterations those fluid and solid solutions exist. Therefore, if the coupling between fluid and solid problems are not stable and robust, the whole FSI problem can take enormous time to solve or it may never converge. So it is very critical to design an efficient and robust coupling algorithm for partitioned solvers.

In the past, several contributions were made in order to create a more stable and robust incompressible partitioned FSI solvers. These include artificial compressibility [11] [12], Robin transmission conditions [13], computation of exact interface Jacobians [14]. Computation of exact interface Jacobians has been demonstrated to be stable as much as monolithic methods. However, all these methods require access to the source code of both fluid and solid solvers in order to be implemented, which is a drawback.

In order to achieve true modularity and freedom in selecting fluid solver and solid solver in partitioned FSI problems, "black-box" solvers are required. Black box schemes do not require any access to fluid and solid solvers's source codes because they work by using the input and output data of them. Although this approach has advantages on its own, the capability of such solvers are limited and depends on the complexity of the problem. One of the earliest method still being used today is fixed-point iterations with dynamic relaxation. After fixed-point iterations, several other methods were developed such as reduced order models, space mapping methods, using higher order polynomials to estimate interface positions and approximate quasi-Newton(QN) methods. Among those methods, QN methods approximate the

interface Jacobians instead of evaluating the exact Jacobians, have shown a better way to provide robust and efficient black box solver alternative.

The current "state of the art" black box coupling method is the "interface quasi-Newton method for approximation of the Jacobians using Least-Squares" (IQN-LS) of [15]. IQN-LS constructs approximate Jacobians by using observations of the interface results and it has been shown that IQN-LS coupling scheme is capable of solving wide variety of strongly coupled FSI problems very efficiently.

Although IQN-LS is deservedly the state of the art implicit partitioned FSI solution scheme due to its performance among others, there is a major problem in the field of partitioned FSI coupling algorithms that when the problem domain is fully enclosed, incompressible and bounded by the DN conditions, partitioned schemes have difficulties on their convergence. The situation is defined and stated by [2] as "incompressible dilemma". Common examples of this dilemma include balloon inflation problems, flow through 3D tubes or even in quasi-enclosed problems as in flow through opening and closing heart valves.

In order to simulate blood flow through arteries, which are inherently fully enclosed 3D pipe problems and the simulations of blood flow in arteries requires FSI application in order to have a much better approximations to the solution, we used the state of the art FSI coupling algorithm IQN-LS for our blood flow simulation. In addition, we explored using artificial compressibility(AC) on the interface boundary in order to improve our blood flow FSI simulations. Artificial compressibility(AC) has been proposed as a solution to the incompressibility dilemma and due to the fact that AC solution fits perfectly with the nature of black-box solvers. Artificial compressibility is a scalar source term added to the continuity equation of the fluid solver. Therefore implementing AC to a production ready FSI flow solver is relatively the least intrusive technical achievement. That's why we tried to implement AC into our IQN-LS FSI solver for our blood flow simulations. However, we couldn't manage to have it worked correctly with the IQN-LS FSI solver at our hands. Nonetheless, we briefly present artificial compressibility in this report and explain the challenges implementing it into a FSI solver.

The outline of the remainder of the thesis is as follows. In chapter 2, we briefly describe fluid and solid domain problems by giving the governing equations in weak form. Chapter 3 outlines many design properties of a FSI problem and describe the necessary building blocks in partitioned FSI solver. In Chapter 4, we investigate the state of the art partitioned FSI coupling scheme, IQN-LS, as well as Aitken's dynamic relaxation method which is the predecessor of IQN-LS and also used solvers based on both algorithms to solve famous benchmark case [1] in order to analyze performance differences between coupling algorithms. Lastly, we briefly describe artificial compressibility(AC) method and present the challenges implementing it. In Chapter 5, we used IQN-LS FSI solver in order to simulate blood flow through arteries and analyzed the results we obtained from the simulation. In last chapter, we will give our conclusions and recommendations about the future of FSI coupling algorithms and their applications on blood flow and hemodynamics problems.

2. DESCRIPTION OF THE FLUID AND STRUCTURE SUBPROBLEMS

The aim of this chapter is to introduce the fluid and structural subdomains, briefly. Since we focused on black-box field solvers in the partitioned FSI coupling, both fluid and structural solvers do not use any particular formulation on their sub-fields.

Both fluid and structural sub-problems belong to the general field of continuum mechanics. Although, they both share several commonalities, they are defined in two different reference frames: an Eulerian formulation for the fluid domain and a Lagrangian formulation for the structural domain. In general, the finite volume method (FVM) for the fluid problems and the finite element method (FEM) for the structural problems are used to solve their respective field equations. Both FVM and FEM are the subset of the more general class of weighted residual methods. Nevertheless, both methods are very popular numerical methods for approximating the solutions of partial differential equations.

In this thesis, foam-extend-3.2 is used for both fluid domain solutions and structural domain solutions. The following two sections will briefly describe general governing equations of both domains.

2.1 Fluid Subdomain

The fluid flow domain is governed by the Navier-Stokes (NS) equations. These equations, typically, are expressed in an Eulerian reference frame, where fluid flows through a fixed spatial discretization. However, in FSI applications, the fluid domain needs to be adaptive for the solid domain deformation because of the interaction between both domains. There are numerous ways to deal with this problem. One of them is to accommodate the deforming boundary by displacing the fluid boundary and its internal discretization via mesh movement algorithms. In order to use such mesh movement algorithm, Navier-Stokes equations has to be casted in an arbitrary Lagrangian-Eularian (ALE) reference frame, an approach first described by [16] and still used on most FSI formulations.

On a fluid domain Ω_f, the governing equations for a viscous, isothermal, incompressible and isotropic Newtonian fluid flow in an ALE reference frame are given by

$$\frac{\partial \mathbf{u}}{\partial t} + (\mathbf{u} - \mathbf{u}_m) \cdot \nabla \mathbf{u} = \nabla \cdot \sigma_f + \mathbf{b}_f \text{ , in } \Omega_f \tag{2.1}$$

$$\nabla \mathbf{u} = 0 \text{ , in } \Omega_f \tag{2.2}$$

Here $\mathbf{u}$ is the fluid velocity, $\mathbf{u}_m$ the ALE coordinate system velocity at a given reference position, σ_f the fluid Cauchy stress tensor and $\mathbf{b}_f$ refers to the body forces acting on Ω_f. For a Newtonian incompressible fluid, the constitutive relation is

$$\sigma_f = -p\mathbf{I} + 2\mu\mathbf{D} \tag{2.3}$$

where p is the thermodynamic pressure, μ the fluid viscosity and $\mathbf{D}$ the rate of deformation tensor. Substituting 2.3 into equation 2.1 and arranging terms gives

$$\frac{\partial \mathbf{u}}{\partial t} + (\mathbf{u} - \mathbf{u}_m) \cdot \nabla \mathbf{u} + \nabla p - \nu \nabla^2 \mathbf{u} = \mathbf{b}_f \text{ , in } \Omega_f \tag{2.4}$$

where ν is the kinematic viscosity and p refers to the kinematic pressure. The formulation 2.4 has the same form used in foam-extend-3.2 software which we use during our studies.

In order to solve the equations, appropriate boundary conditions are required. Dirichlet-Neumann boundary conditions along the fluid boundary can be posed as

$$\mathbf{u} = \mathbf{u}_0 \text{ , on } \Omega_{f,D} \tag{2.5}$$

$$\mathbf{n} \cdot \sigma = \mathbf{t} \text{ , on } \Omega_{f,N} \tag{2.6}$$

where $\mathbf{n}$ is the unit normal outward pointing vector. From these two boundary conditions, other boundary conditions can be derived.

2.2 Solid Subdomain

In our simulations, linear elastic stress analysis structural solver was coupled with the incompressible, Newtonian, viscous fluid solver. The governing equations of the structural solver used described by [17] are as follows. For a solid body element, the momentum balance states the following equations:

$$\frac{\partial^2 (\rho \mathbf{u})}{\partial t^2} - \nabla \cdot \sigma = 0 \tag{2.7}$$

8

where $\mathbf{u}$ is the solid displacement vector, ρ is the density and σ is the stress tensor with the assumption of free body force.

In order to complete the governing equations, following constitutive relation must be specified

$$\sigma = 2\mu\varepsilon + \lambda tr(\varepsilon)\mathbf{I} \tag{2.8}$$

where $\mathbf{I}$ is the unit tensor. μ and λ are Lamé parameters, material properties. Lastly, the strain tensor ε is defined in terms of $\mathbf{u}$ as follows,

$$\varepsilon = \frac{1}{2}[\nabla\mathbf{u} + (\nabla\mathbf{u})^T] \tag{2.9}$$

By combining all three equations, the governing equation for linear elastic solid body can be written as

$$\frac{\partial^2(\rho\mathbf{u})}{\partial t^2} - \nabla\cdot[\mu\nabla\mathbf{u} + \mu(\nabla\mathbf{u})^T + \lambda\mathbf{I}tr(\nabla\mathbf{u})] = 0 \tag{2.10}$$

Notice that the equation 2.10 is written with only one unknown $\mathbf{u}$. There is also another important point that the three displacement components are coupled. In order to overcome this issue, the solver in foam-extend-3.2, follows the "segregated manner", where each displacement component is solved separately and the inter component coupling is treated explicitly with several iterations for recovery.

9

3. FSI PRELIMINARIES

In this chapter, the building blocks of a partitioned FSI solver is investigated. All the following sections contains general information about the partitioned FSI coupling so that this chapter would be a foundation for the following chapters.

3.1 FSI Problem Description

The term "fluid-structure interactions" refers to a two-field problem of interaction between fluid flow and deformable structural bodies. In most FSI problems, a fluid flow induces pressure to a near deformable structure and in return deformed structure response to the fluid flow by changing its boundaries which also affects the fluid flow. Therefore, FSI problems describes two field coupled domains where each sub domain have significant influence on the other. In a typical single field mechanics problem such as fluid-only or structure-only, a set of governing differential equations on a domain and a set of boundary conditions on that domain would be enough. However, in FSI, boundaries are in motion so that the boundary conditions on both fluid domain and structure domain must be satisfied simultaneously. Since fluid domain and structure domain do not overlap, a meaningful coupling between fluid-structure interface must also be designed.

The notional FSI problem for an arbitrary volume is depicted in 3.1, with a fluid domain given by Ω_f, solid domain, Ω_s and associated boundaries $\partial \Omega_{f,s}$. The two sub-domains are independent from each other, and interact only along a common and shared interface Γ, where $\Gamma = \Gamma_s = \Gamma_f$. The FSI problem requires that both the kinematic and dynamic continuity be satisfied at all times along the shared interface $\Omega_{f,s}$.

Kinematic continuity at the interface $\Omega_{f,s}$ ensures mass conservation, whereas dynamic continuity ensures conservation of linear momentum. Therefore both kinematic continuity and dynamic continuity must be satisfied on the coupling interface.
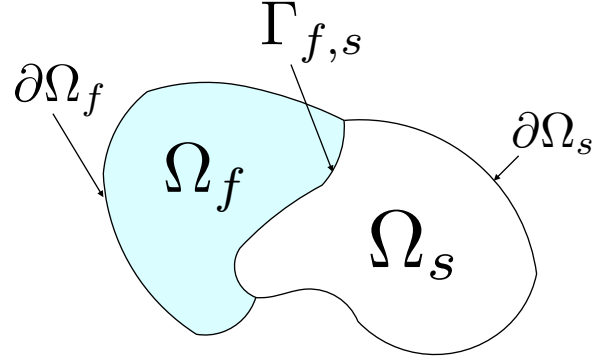
Figure 3.1 : FSI problem description, depicting the fluid and solid domains, sharing a common interface Γ

Kinematic continuity states that the fluid flow velocity at the interface $\mathbf{u}_{f,\Gamma}$ equals the boundary velocity as described in 3.1.

$$\mathbf{d}_{f,\Gamma} = \mathbf{d}_{s,\Gamma} \tag{3.1}$$

Dynamic continuity states that stresses from both fluid and solid are equal at the interface

$$\sigma_{s,\Gamma} \cdot \mathbf{n}_{s,\Gamma} = p_{f,\Gamma}\mathbf{n}_{f,\Gamma} - \tau_{f,\Gamma} \cdot \mathbf{n}_{f,\Gamma} \tag{3.2}$$

where $\mathbf{n}_s$ and $\mathbf{n}_f$ are the respective interface normals. Here $\sigma_{s,\Gamma}$ indicates the solid stress state, $\tau_{f,\Gamma}$ the fluid viscous stress tensor and $p_{f,\Gamma}$ the interface pressure.

In this thesis, Dirichlet-Neumann(DN) interface boundary conditions were used. Dirichlet boundary (displacement) imposed along the fluid interface Γ_f, and Neumann interface is applied to the solid domain interface Γ_s in the form of pressures and shear stresses.

3.2 Monolithic vs. Partitioned Solution Schemes

There are two major FSI coupling approaches which are monolithic and partitioned.

In monolithic coupling also called strongly-coupled, governing equations for both fluid and structure subdomains are cast in terms of the same primitive variables. In other words, a new governing equations are derived by using both fluid equations and structure equations which would then be applied on the same level of discretized mesh interface. Consequently, the equations of fluid, structure and mesh moving are solved simultaneously at the same time step. In order to accomplish that *Arbitrary Lagrangian-Eulerian (ALE)* formulation can be used. To use ALE

12

formulation in a FSI problem, advanced mesh update techniques must be deployed in order to adapt changing boundaries of the domains as well as depending on the discretization parameters, special predictor-multicorrector algorithms and interface projection techniques for non-matching fluid and structure interface discretisations must also be implemented [18], [19] and [20].

Due to fully-coupled fashion, monolithic solvers are more robust than partitioned-coupled solvers. However, monolithic solvers must be designed from scratch by virtually precluding fluid and structure solvers. There are three categories of coupling techniques in strongly-coupled FSI methods which are *block-iterative*, *quasi-direct* and *direct-coupling*. In all three coupling techniques, iterations are performed within a time-step to simultaneously converge the solutions of all the equations involved [8].

In partitioned coupling, both fluid and structure domains are modeled and discretized separately. On the fluid part, traditional CFD techniques are used for the flow properties. On the structure part, finite element on structural mechanics are applied. Therefore, existent fluid solvers and structure solvers can be used which make this approach very flexible and desirable. However, stress and displacement terms must be transferred across the domain interface. Moreover, this coupling between fluid solver and structure solver must produce accurate results without deteriorating the convergence of the system significantly. Meeting with those criteria are the hardest part of partitioned coupling in FSI.

As mentioned before, using production ready, optimized, robust existing solvers for both fluid domain and solid domain has been very attractive, which led to more different kinds of partitioned coupling methods where all of them tried to improve stability, robustness and convergence of partitioned coupling. Notice from figure 3.2, majority of FSI coupling developments has been made for partitioned coupling methods. There are two types of partitioned solution schemes, explicit and implicit. In explicit schemes, the fluid and the solid sub-domains are solved in a staggered fashion with no convergence or residual checks. That is why, explicit schemes or loosely coupled schemes are not stable enough to solve strongly coupled FSI problems where large deformations or high "added mass effect" happens. On the other hand, explicit schemes have been used in aeroelasticity problems successfully. In such problems, the
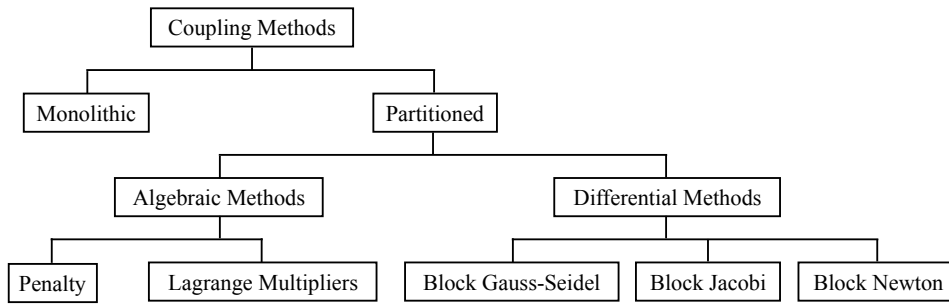
Figure 3.2 : Summary of FSI coupling approaches, reproduced from [21]

solid to fluid density ratios are large which results in a weakly coupled system. For the class of problems with large deformations or with high nonlinearity or with high "added mass effect", implicit methods becomes important because with improvements, those problems can be solved successfully.

In conclusion, black box solvers are attractive enough to warrant additional research because they increases the efficiency of development time.

3.3 Partitioned FSI Solver

3.3.1 Fluid and solid solvers

In this thesis, foam-extend-3.2 [22] is used, a special version of open source CFD software OpenFOAM [23] , to solve both fluid equations and solid equations. The associated governing equations were described in Chapter 2.

foam-extend-3.2 is an open-source object oriented library for numerical solution of partial differential equations. It is a fork of OpenFOAM and maintained by academia which leads to more diverse and advanced capabilities over the official version. It is being developed by using high level C++ functionality. It comes standard with large number of utilities and solvers. Despite being and open source, it has comparable capabilities to most high-end commercial CFD softwares.

The solvers are categorized according to their fluid problem properties. In this thesis, fsiFoam [24] solver from extend-bazaar toolkit is used. It is a incompressible partitioned FSI solver and it couples icoFoam and stressFoam solvers. icoFoam solver is a fluid solver which uses finite volume method in order to solve incompressible,

Newtonian, laminar transient flow. stressFoam solver is a solid solver which also uses finite volume method to solve nonlinear material models.

3.3.2 Implicit iterative coupling

In order to improve accuracy and stability of partitioned solvers, implicit coupling in which coupling iterations are performed in a given time step. Implicit coupling scheme workflow is illustrated in figure 3.3(b). As can be seen from the figure 3.3(b),
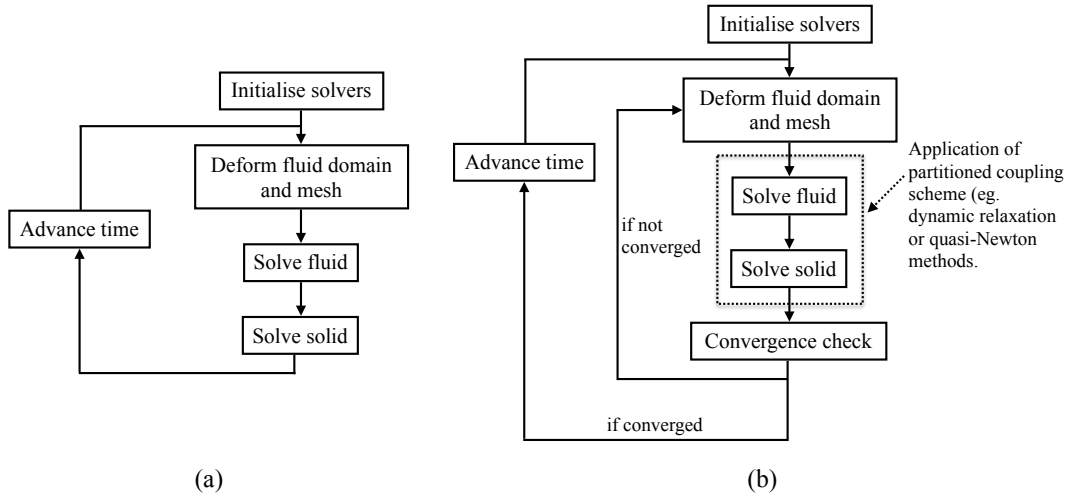

(a)   (b)

Figure 3.3 : (a) weak coupling(explicit), (b) strong coupling(implicit)

in implicit coupling, due to the nature of staggered approach, there is a natural time lag between serial fluid and serial solid solutions. Therefore, to minimize the numerical errors derive from this time lag, the following convergence criterion

$$\frac{|\mathbf{d}_{\Gamma,k+1} - \mathbf{d}_{\Gamma,k}|}{\sqrt{m}} \leqslant \varepsilon, \tag{3.3}$$

where subscript k indicates the iteration counter, ε indicates the error tolerance. m indicates the total number of DOFs along the discrete interface and it removes the mesh size dependencies from the convergence criterion.

3.3.3 Mesh movement

In FSI problems, dynamic mesh techniques play key role in the performance of the solvers because by using dynamic mesh updates and mesh refinements on the fly would preserve the mesh quality, thus also protects the stability and convergence of the solution. Although dynamic mesh mechanism on the fly is not enough solely in FSI solvers, they are a must even in small displacement cases.
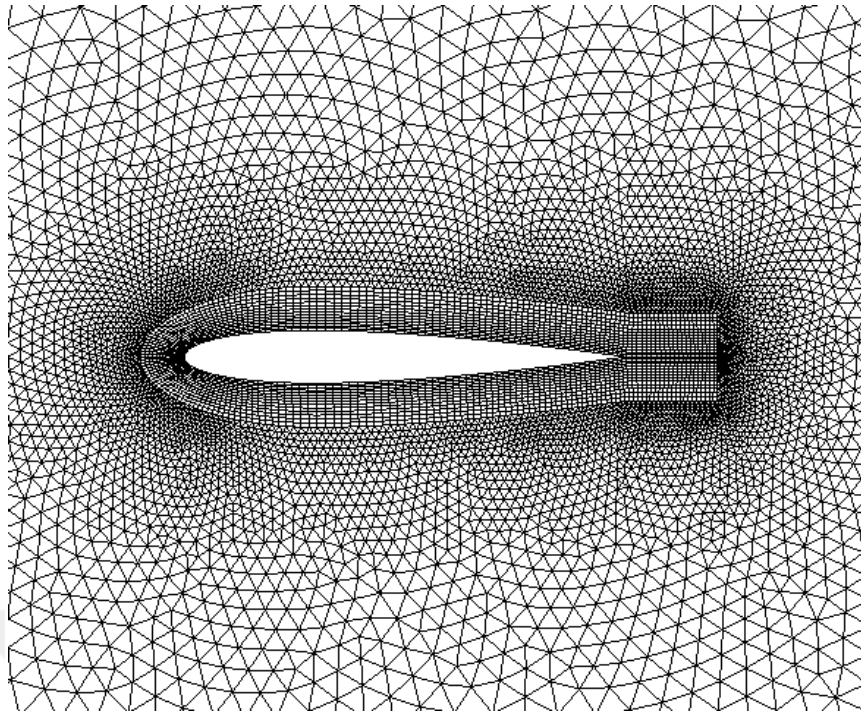
Figure 3.4 : An example of Dynamic Mesh application

Dynamic Mesh technique implemented in OpenFOAM is capable of refining mesh and updating the meshes on subdomains automatically. Since the mesh motion cannot be know priori, a mesh motion equation must be defined in order to solve moving mesh during the given time-step of FSI solver. There are 4 simple mesh motion equation present in OpenFOAM :

1. Spring analogy: insufficiently robust

2. Linear + torsional spring analogy: complex, expensive and non-linear

3. Laplace equation with constant and variable diffusivity

4. Linear pseudo-solid equation for small deformations

In fsiFoam solver, mesh motion model relies on Laplace equation with constant and variable diffusivity. Diffusion of the boundary mesh displacement to the internal parts of the solution domain is modeled as

$$\nabla(\gamma\nabla\mathbf{d}) = 0 \tag{3.4}$$

where γ is the displacement diffusion coefficient, and $\mathbf{d}$ is the point displacement field. The rate of diffusion of the displacement from the boundaries to the internal mesh

regions is defined with the spatially varying diffusion coefficient γ given as a function of the distance between the point **x** and the mesh boundary as,

$$\gamma = \gamma(r) \tag{3.5}$$

where r is the distance between the mesh point and the mesh boundary and the coefficient function is prescribed in a way that makes the coefficient decrease with the distance from the boundary, in order to reduce the displacement. The solution of the equation 3.4 is approximated by using the FEM thanks to its implementation in foam-extend-3.2.

4. BLACK-BOX PARTITIONED FSI COUPLING

4.1 Introduction

In this chapter, we introduce the most popular black box partitioned FSI coupling algorithms. We investigate the algorithms and compare their performances in test cases. In addition, explicit scheme and implicit scheme FSI solvers are described in detail.

4.2 Explicit Scheme

Explicit scheme is one of the earliest black box solution scheme applied in partitioned FSI solvers. This algorithm has been classified as loose-coupling or weak coupling due to the fact that the algorithm does not test any convergence on the FSI coupling iteration. The lack of any control in FSI coupling makes explicit scheme coupling vulnerable to the problems with high "added-mass effect" or with strong interactions. Nonetheless, due to the weak nature of aeroelasticity problems, this algorithm can still be used today in those problems with success [3].

In loose-coupling, the equations of fluid mechanics, structural mechanics and mesh moving are solved sequentially as in Figure 4.1.

As it can be seen from the Figure 4.1,

1. Dynamic mesh solver updates the mesh according to the displacement at the structure part and velocity at the interface is extrapolated from the rate of displacement.

2. Fluid mechanics equations are solved by using that received values from the extrapolation.

3. Structural mechanics equations with the updated fluid mechanics interface traction are solved.
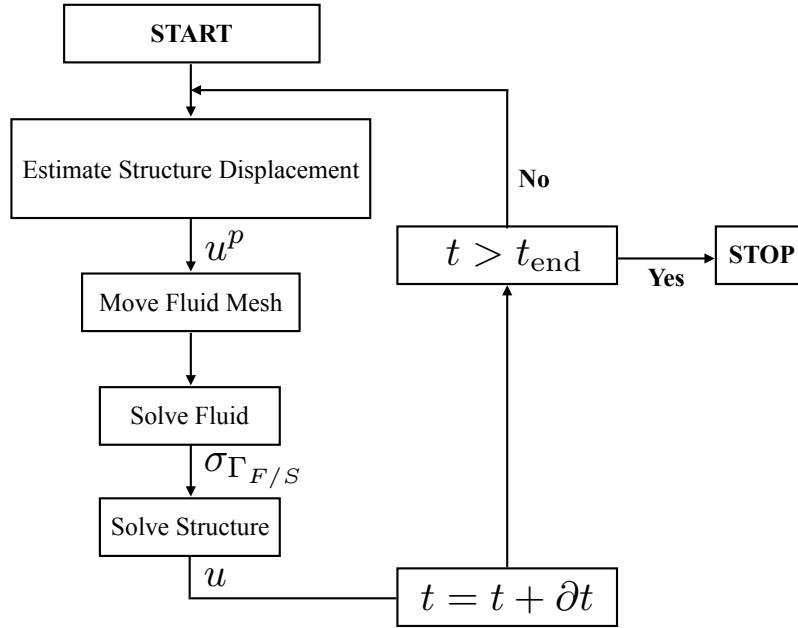
19

Figure 4.1 : Loose-Coupling solver sequence

4. By using the new displacements from structure solver, mesh moving algorithm updates the meshes.

Although this type of solver looks very promising, there is a significant stability issue that must be handled carefully. The origin of the problem is whether the following equality,

$$u^p = u \tag{4.1}$$

where u is the velocity of the interface boundary, u^p is the predicted interface boundary velocity, holds.

In other words, the new fluid forces are calculated by using the predicted(extrapolated) displacements instead of the actual displacements due to the mesh update at the end of the solver. Consequently, an "added mass" problem is encountered during the solutions. Inaccuracy of the extrapolation approximation of the displacements, fluid flow solver encounters with an added mass input to the system which in turn affects the convergence significantly. Moreover, decreasing time step does not improve the stability derived from the added mass. According to the previous works, when

$$\frac{fluid\ density}{solid\ density} >= 1 \tag{4.2}$$

significant instabilities on the solution were observed [25], [9].

20

4.3 Coupled FSI Problem

In this section, definitions of the functions that represent flow solver and structural solver, as they are used by fixed-point methods, are given. The governing equations of both flow solver and structural solver are given in chapter 2. The following function definitions are taken from [15].

Dirichlet-Neumann decomposition of the FSI problem imposes velocity on the fluid side of the interface and stress distribution on the structural side of the interface. The following abstractions emphasize that the solvers are treated as black boxes.

The function

$$\mathbf{y} = F(\mathbf{x}) \tag{4.3}$$

is referred to as the flow solver. It describes the relationship of flow solver as a black box solver in the sense that the discretized position $\mathbf{x} \in \Re^u$ is given to the flow code and returns the new calculated stress distribution $\mathbf{y} \in \Re^w$ on the interface.

The function

$$\mathbf{x} = S(\mathbf{y}) \tag{4.4}$$

is referred to as the structural solver. It also describes the relationship of structural solver with the interface, where structural solver takes the stress distribution from the interface and calculates the new position of the fluid-structure interface. With these definitions, the FSI problem is given by

$$\mathbf{x} = S \circ F(\mathbf{x}) \text{ or } R(\mathbf{x}) = S \circ F(\mathbf{x}) - \mathbf{x} = 0, \tag{4.5}$$

in fixed-point or root finding formulation, respectively, with R being the residual operator.

4.4 Aitken's dynamic relaxation

Aitken's dynamic relaxation, also called tight coupling, is a convergence accelerator technique used in fixed point iterations. As defined in the previous section, black box FSI solvers can be defined in a way that the problem becomes fixed point iteration which aims to find the appropriate interface boundary deformation [26].

In tight coupling, an outer fixed-point iteration is used in order to ensure the convergence at every given time-step. In order to accomplish this, well-known Aitken

Method which is a scalar relaxation factor, determined dynamically, injected into the fixed-point iterations as can be seen from the Figure 4.2 is used. By using a relaxation multiplier the effects of the extrapolation is minimized so that the stability and the rate of convergence are improved.
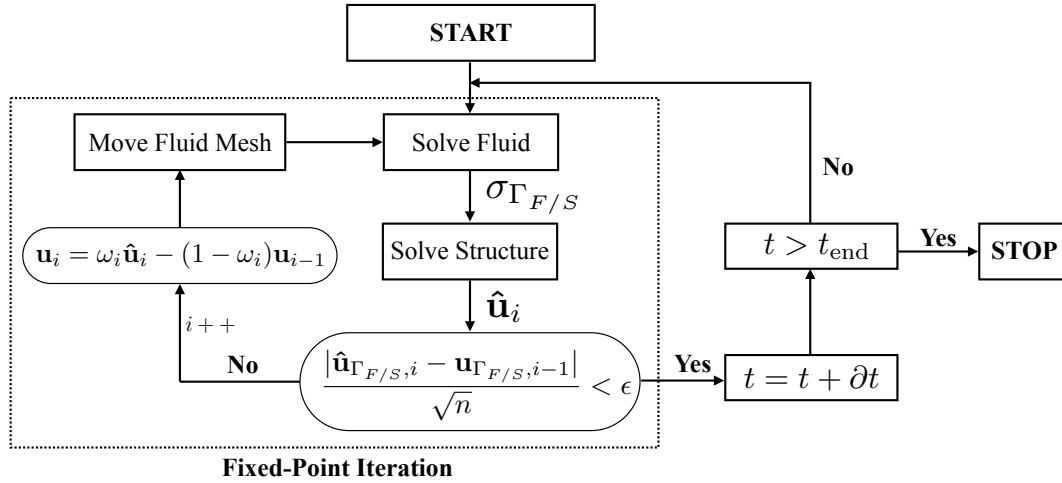

Figure 4.2 : Tight-Coupling solver sequence with fixed point iteration and dynamic relaxation

The algorithm of the tightly-coupled solver can be described as:

1. Solve the mesh equation

2. Transfer interface velocity to fluid solver

3. Solve the flow equations

4. Transfer interface pressures into structure solver

5. Solve the structure equations

6. Restrict new interface deformations by using under-relaxation

7. Check the residuals between the last time step and the new one

As in the loosely-coupled solver, existing fluid and structure solvers can be used and a better stability and convergence can be achieved by using tightly-coupled solvers.

4.5 IQN-LS

IQN-LS is "the state of art", implicit partitioned FSI coupling method. It uses quasi-Newton method on the interface boundary and approximation of Jacobians are determined by using least squares method as described in [15]. The method is based on reduced order model, [27], of fluid solver. Therefore, by calculating the first response data from fluid solver on the interface boundary movement can be gathered and a reduced order model for the fluid can be established. Since creating reduced order model during the coupling iterations have negligible computational cost, this method improves performance of black box implicit partitioned FSI coupling solvers.

The reduced order model are built up during the coupling iterations. These reduced order models enhance the convergence of fixed point iterations. The complete algorithm taken from [15] is as follows.

At each time step and during the fixed point iterations, assume that fluid solver called k times, then for k interface positions $X_i^f, i = 1, \ldots, k$, k corresponding stress distributions at the interface $P_i^f, i = 1, \ldots, k$ are computed by the fluid solver. With this information a matrix

$$V = [\Delta X_1^f, \ldots, \Delta X_j^f, \ldots, \Delta X_{k-1}^f] \tag{4.6}$$

with displacement modes of the interface $\Delta X_j^f = X_j^f - X_k^f, j = 1, \ldots, k-1$ and a matrix

$$W = [\Delta P_1^f, \ldots, \Delta P_j^f, \ldots, \Delta P_{k-1}^f] \tag{4.7}$$

with the corresponding changes in stress distribution at the interface $\Delta P_j^f = P_j^f - P_k^f, j = 1, \ldots, k-1$ are constructed. With these two matrices, an arbitrary displacement ΔX^f and the corresponding change in stress distribution ΔP^f can be approximated by a linear combination of the computed modes as follows:

$$\Delta X^f \approx V \alpha \Delta P^f \approx W \alpha \tag{4.8}$$

with $\alpha = [\alpha_1, \ldots, \alpha_{k-1}]^T$. Minimizing $\| \Delta X^f - V \alpha \|$ results in a least squares problem with solution

$$\alpha = (V^T V)^{-1} V^T \Delta X^f \tag{4.9}$$

so that

$$\Delta P^f = F_X^k \Delta X^f \tag{4.10}$$

23

$$F_X^k = W(V^TV)^{-1}V^T. \tag{4.11}$$

The resulting reduced order models for the fluid solver and in a similar way for the structural solver are

$$P = P_k^f + F_X^k(X - X_k^f) \tag{4.12}$$

$$X = X_k^s + S_P^k(P - P_k^s) \tag{4.13}$$

By using the reduced order model for the fluid problem, the structural problem can be solved with Newton-Raphson iterations upon convergence as follows:

$$G(X^{l+1},P^{l+1}) \approx G(X^l,P^l) + (\frac{\partial G}{\partial X} + \frac{\partial G}{\partial P}F_X^k)(X^{l+1} - X^l) = 0 \tag{4.14}$$

with l the iteration level for the Newton-Raphson iterations. The simplified representation of the algorithm can be seen in figure 4.3.
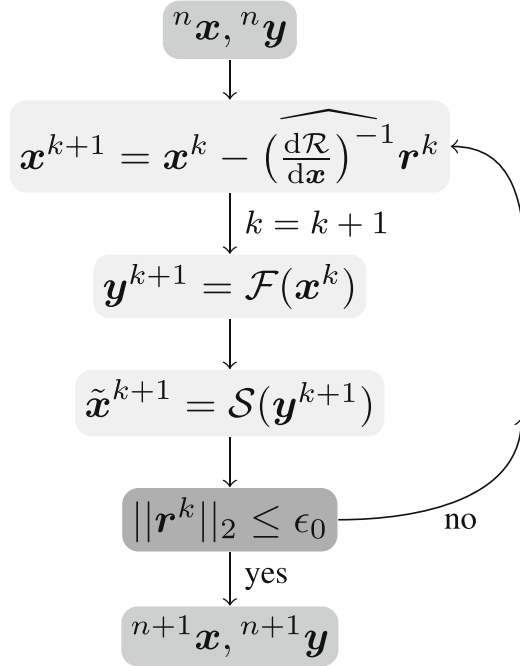

Figure 4.3 : Simplified representation of IQN-LS algorithm taken from [28]

4.6 Flow Induced Oscillating Flexible Beam Benchmark

In this section, partitioned FSI solvers mentioned in this chapter was used to run on a benchmark case. Both Aitken's relaxation method and IQN-LS method are used in order to investigate their performances on this benchmark case. By running this case with both algorithms, we confirmed that the partitioned FSI solver implemented

in fsiFoam are setup correctly and performed as expected. Nonetheless, performing these tests give us a deeper understanding about the nature of algorithms, their implementation details and also the post processing techniques. At last, with a robust and stable implementation of IQN-LS solver at our hands, we can build upon on it.

Flow induced oscillating flexible beam case is a well-known 2D FSI benchmark case [1]. As it can be seen from figure 4.4, a linear elastic beam is fixed into a sphere inside a fluid flow domain. The flow comes from the inlet goes around the sphere and in the course of time Von Karman vortex street is formed during the simulation. Due to the pressure change induced by the vortexes, beam starts to oscillate. This problem is counted as large deformation FSI due to the fact that during the simulation, the beam's edge towards to the outlet displacement is relatively large.
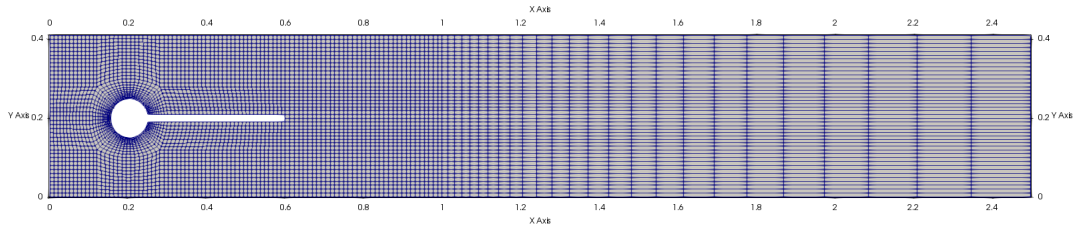

Figure 4.4 : Benchmark geometry and mesh

Table 4.1 : Hron-Turek Mesh Properties

Stats/domain	Fluid Mesh	Solid Mesh
points	11134	1484
faces	21575	2631
cells	5336	630
boundary patches	7	3
hexahedra elements	5336	630
Max aspect ratio	17.2499	4.5
Max skewness	0.409801	1.49568e-08

The mesh properties in our test case setup is given in table 4.1. As it can be seen from the table, the discretization is relatively small. There are around 6000 cells combined from both fluid and solid domain, and all of the cells are made of hexahedra elements which are known to be good for convergence in FVM simulations.

Since FSI coupling is very hard to solve numerically, starting to the simulation with the highest quality of mesh is a rule of thumb. As it can be seen from the table 4.1, maximum aspect ratio and maximum skewness of both domain's meshes are in good shape.

Maximum aspect ratio is very important on FVM simulations, because it indicates the ratio between the largest face size to the smallest face size, which in turn determines directly the gradient calculations of the field in FVM.

On the other hand, maximum skewness is also prominent indicator about the quality of meshes. Skewness ratio refers to the angle ratios between the individual mesh cells. Since FVM method in OpenFOAM is cell based, the face values are calculated from the midpoint of each cells by interpolation. With high skewness, the interpolation calculations would impose numerical errors into the simulation.

Both maximum aspect ratio and maximum skewness have an important role in the convergence of CFD simulations, due to the fact that they directly effect the numerical stability.
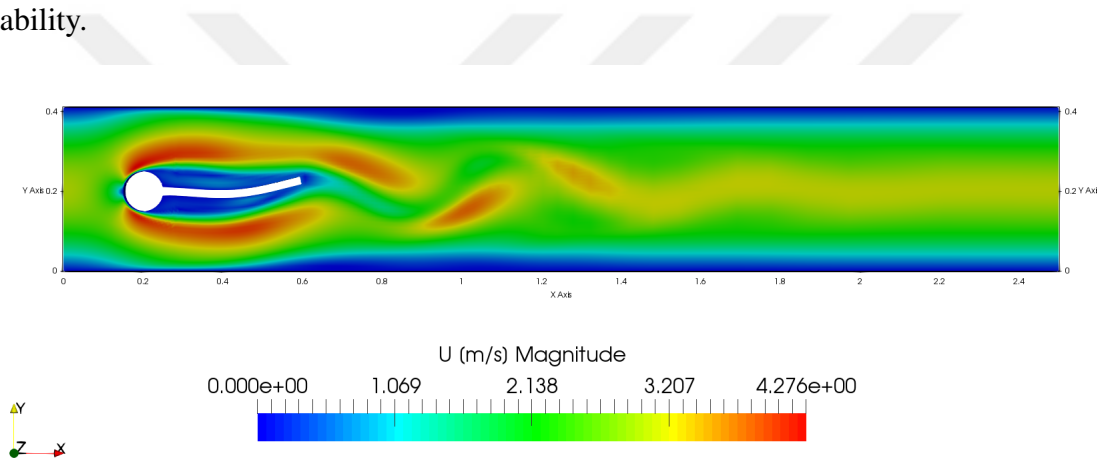

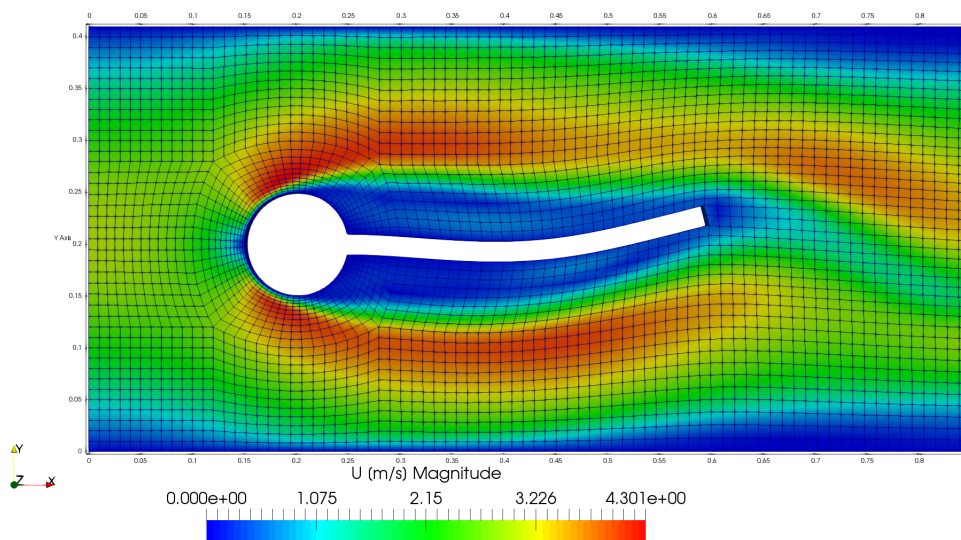**Figure 4.5** : At time step=5.78, steady state fluid velocity contours

Figure 4.6 : At time step=5.78, steady state fluid velocity contours, enlarged view

In figure 4.5 and also 4.6, the so-called von Karman vortex street can be seen. The reddish droplet like shapes indicates the fluid which flows faster than other colors. The

26

figure was taken at time = 5.78 seconds and it depicts the steady state of the simulation. Also from the same figure, the no-slip boundary condition which states that the velocity of fluid is 0 can be seen. The darkest blue shade indicates the zero velocity of fluid and on the fluid domain boundary, it is all dark blue. The same blue can also be seen on the tip of the sphere and also in the wake area of it where velocities are decreased.

The deflection on the tip of the beam with corresponding coordinates $(x, y, z) = (0.60.20.025334)$ can be seen in figure 4.7. It shows that the deflection was large in both x and y axis. The large deflection derives from the fact that high magnitude forces were applied which was measured in figure 4.8.
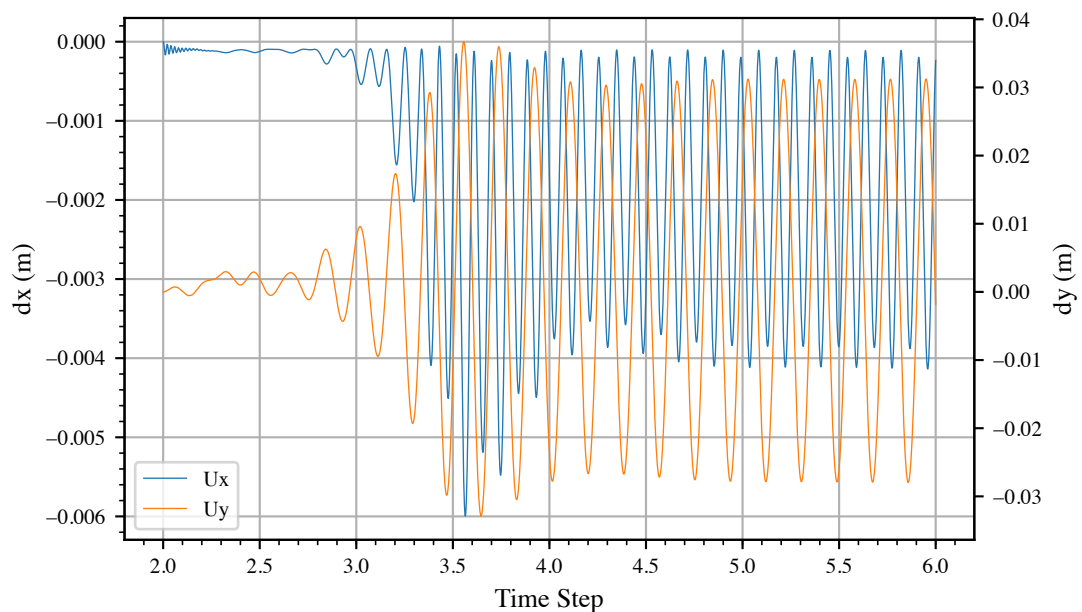

Figure 4.7 : Deflection vs Time at the the tip of the beam with the coordinates (x, y, z) = (0.6 0.2 0.025334)

In figure A.3 and A.4, the convergence and stability analysis of the simulation can be made. In CFD simulations, the Courant number and keeping it under 1 is very crucial in order to reach convergence to the solution. Courant number gives and idea about the accuracy of the simulation. If the time step size is not selected according to the mesh sizes, then the accuracy of the solution may be compromised. Another basic check on any numerical computation is also the residuals of the unknowns. In this simulations, fluid solver solves velocities on both directions and also the structural solver solves the displacements. As can be seen from the residuals graph, initial residuals (indicates the beginning of time steps) are decreasing and they reaches to steady state with very
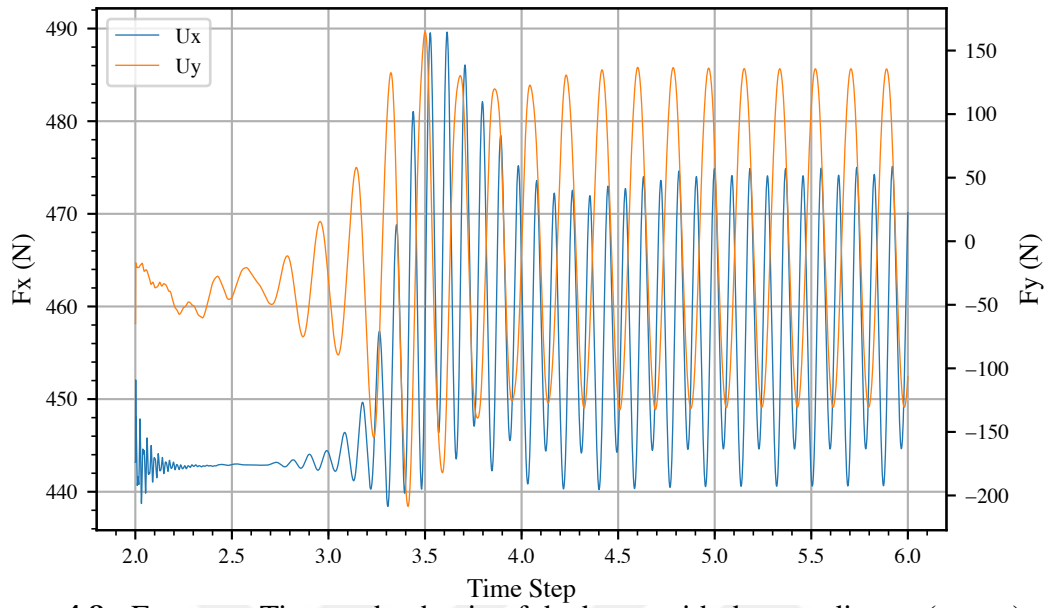
Figure 4.8 : Forces vs Time at the the tip of the beam with the coordinates (x, y, z) = (0.6 0.2 0.025334)
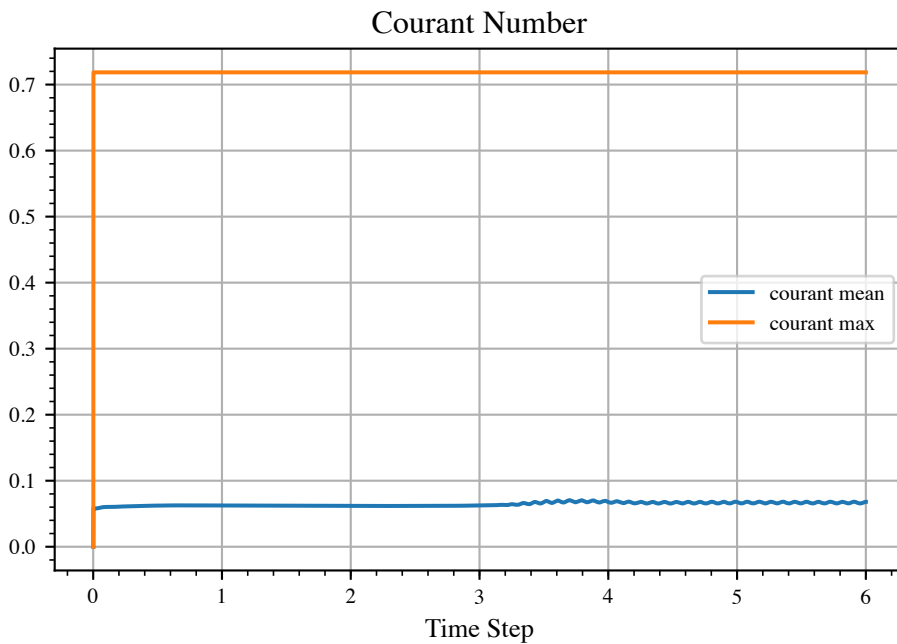

Figure 4.9 : Courant number mean and max value of fluid solver during simulation
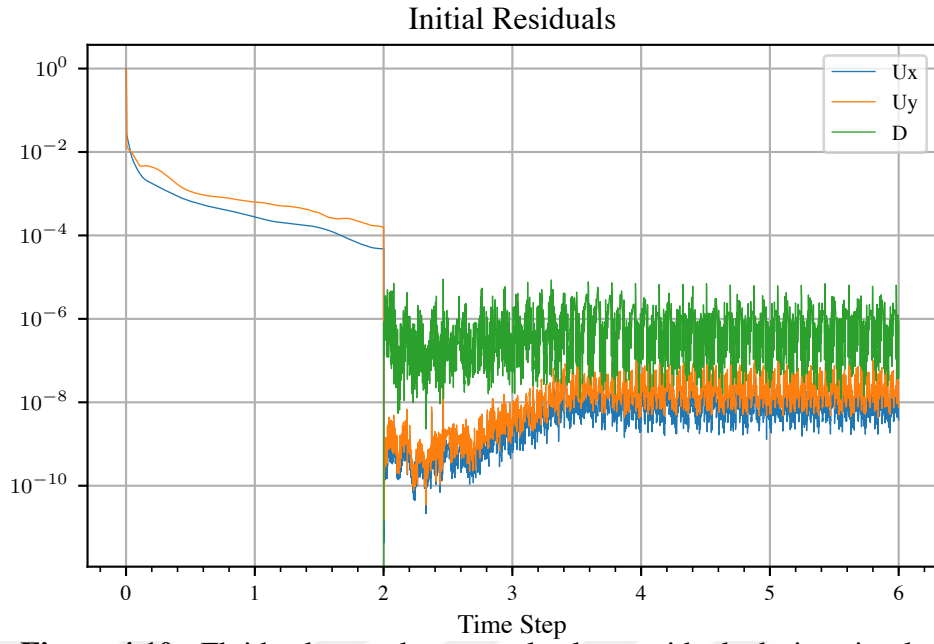
Figure 4.10 : Fluid solver and structural solver residuals during simulation

low errors. To conclude, IQN-LS method in this benchmark worked very well. The simulation was stable, robust and accurate.

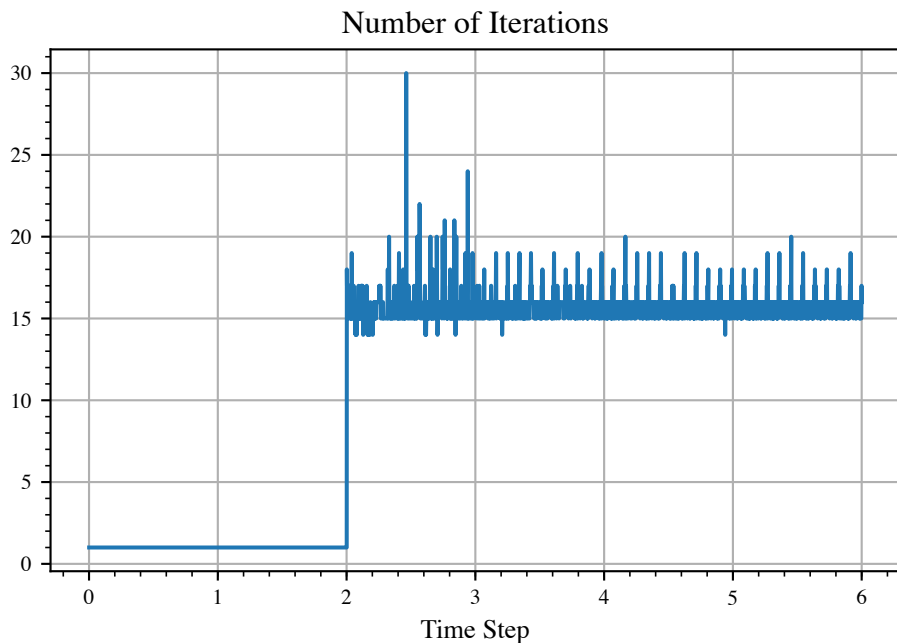**Figure 4.11** : Number of IQN-LS coupling iterations during simulation

In figure 4.11, FSI coupling iterations in every time steps can be seen. Up until $t = 2$, when the vortexes started to be formed and induces pressure differential on the coupling interface, the number of iterations per time step was only one. In other words, there was no movement in this specific test case. But after that, in every time step,

IQN-LS coupling iterates around 15 times in order to maintain Dirichlet-Neumann boundary conditions along the interface boundary.

4.7 Artificial Compressibility and IQN-LS

We study blood flow through arteries and the geometry and nature of the problem can be stated as incompressible flow through fully enclosed 3D pipes. However, there is a technical challenge named "incompressibility dilemma" first stated by [2] of fully enclosed, incompressible fluid in partitioned fluid structure interaction problems. As described by [2], partitioned, incompressible, FSI, based on Dirichlet-Neumann domain decomposition solution schemes cannot be applied to problems when the fluid domain is fully enclosed. Such problems are defined ill-posed numerically which makes finding solutions to them with partitioned FSI solvers harder or even impossible.

In order to handle "incompressibility dilemma", "artificial compressibility (AC)" can be used so that the numerical solutions of such problems become better. AC was originally used in FSI applications in order to remove some of the instabilities related to strongly coupled, incompressible problems [29], [30].

Artificial compressibility is a scalar factor added into the continuity equation in fluid solver, therefore it is relatively easy to implement it into flow solver. AC usually is added into robust compressible solvers in order to give those solvers ability to solve also incompressible flow problems. However, a novel adaptation of this technique applied into FSI problems by [31] and the new FSI solver with AC performed slightly better for fully enclosed incompressible problems. Nonetheless, the same solver also showed performance degradation in other types of problems [31]. Brief description of what AC is, and its usage in a partitioned FSI solver are as follows.

Artificial compressibility modifications to the fluid domain solver are described in this section. The governing equations for a viscous, isothermal, incompressible and isotropic Newtonian fluid flow in an ALE reference frame are given by

$$\frac{\partial \mathbf{u}}{\partial t} + (\mathbf{u} - \mathbf{u}_m) \cdot \nabla \mathbf{u} + \nabla p - \nu \nabla^2 \mathbf{u} = \mathbf{b}_f, \qquad (4.15)$$

$$\nabla \mathbf{u} = 0 \qquad (4.16)$$

Here $\mathbf{u}$ is the fluid velocity, $\mathbf{u}_m$ the ALE coordinate system velocity at a given reference position, ν is the kinematic viscosity, p refers to the kinematic pressure and $\mathbf{b}$ refers to the body forces.

The basic of AC is to modify continuity equation 4.16 by inserting a pressure time derivative such that

$$\beta\left(\frac{\partial p}{\partial t}\right) + \nabla\mathbf{u} = 0, \tag{4.17}$$

where β is the artificial compressibility coefficient. The solution of the modified equation 4.17 can be approximated in a given iteration as follows,

$$\frac{\beta(p_k^{n+1} - p_{k-1}^{n+1})}{\Delta t} + \nabla\mathbf{u}_k^{n+1} = 0, \tag{4.18}$$

where subscript k represents the current FSI coupling iteration in time step $n + 1$ and Δt is the simulation time step size. Therefore, while the incompressible continuity equation 4.16 is initially violated, at convergence for time step $n + 1$, the AC compressibility term disappears as $p_k^{n+1} \to p_{k-1}^{n+1}$, thereby satisfying the original continuity equation.

One of the most critical challenge of integrating AC into a quasi-Newton method is to change pressure component at the coupling interface so that the coupling algorithm (IQN-LS) be aware of the additional pressure sensitivities comes from the fluid domain. Since AC basically applies an under-relaxation into incompressible flow solver's pressure wave, thus decreasing the stiffness of pressure propagation in the fluid domain, it also changes the applied pressure onto the coupling interface. Therefore, while implementing AC into IQN-LS solver, the force difference originated from the AC in flow solver must be taken into account also in the coupling iterations and pressure correction must be applied. Otherwise a Newton-like method with AC/FSI cannot work. More detailed description of this technique can be found in [31].

4.8 Remarks

The individual analysis of flow induced oscillating flexible beam benchmark was done in the previous section. As it can be seen from there, both flow solver and structural solver converged into the solution and numerically gave stable solutions. Here, we compare the number of iterations of FSI coupling algorithms on the same problem as well as how the difference between the number of iterations reflected on the execution times of the simulation.

The advantage of using IQN-LS FSI solver can be clearly seen from the figure 4.12. IQN-LS method converges much more faster than Aitken's relaxation method which in turn completes the simulation in a much shorter time with the same computational resources.
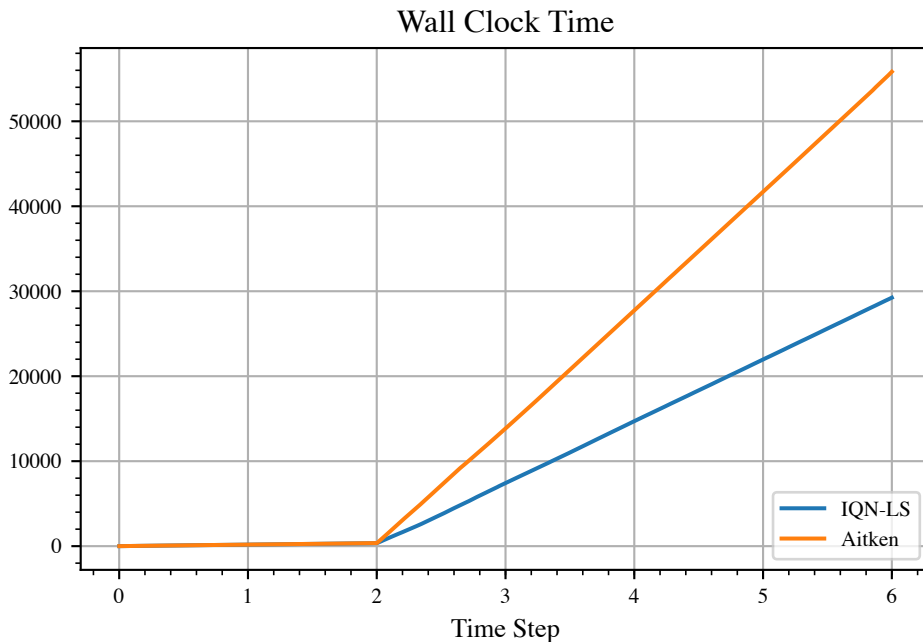

Figure 4.12 : Execution times comparison of FSI coupling methods on flow induced oscillating flexible beam benchmark

In figure 4.13, it can be seen that IQN-LS method needs around half the number of FSI coupling iterations in order to converge within one time step and move onto the next time step. For this benchmark, IQN-LS method performs almost twice as better than Aitken's relaxation.
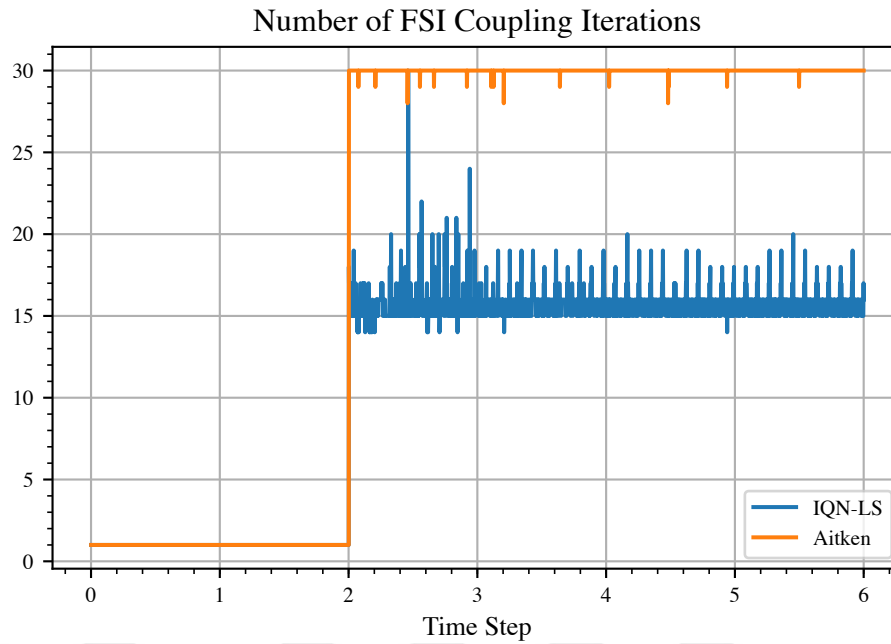
Figure 4.13 : Number of iterations comparison of FSI coupling methods on flow induced oscillating flexible beam benchmark

Another observed difference between IQN-LS and Aitken method on the benchmark case was that while the evaluated deflection at the tip of the beam was almost the same between each method, the forces calculated by the Aitken method showed some noise in comparison with the results of IQN-LS. Look at the figures A.1 and A.2 in the Appendix.

The results found in this chapter are consistent with the results found in [28]. By retesting the same simulation case, we both confirmed them and also be sure about the performances of the solvers and their settings we use. These results gave us a valid reference point before implementing our blood flow through large artery case and analyze its results in detail.

Another finding of this chapter was that there is a challenge in integrating AC into IQN-LS coupling scheme. It was done successfully by [31] for another quasi-Newton based partitioned coupling algorithm and it promised improvement for the fully enclosed cases such as our blood flow through artery problems. However, we could not manage to have AC worked very well in our IQN-LS solver.

5. FSI IN HEMODYNAMICS

5.1 Introduction

In this chapter, we used state of the art partitioned FSI coupling scheme IQN-LS algorithm in order to simulate blood flow through large arteries. Our motivation of using FSI in blood flow in arteries simulations derives from the fact that the Reynolds number at the peak systole characterizes the flow regime and the complexity in the order of several hundreds in cerebral arteries and few thousands in the aortic arteries. Those Reynolds number ranges corresponds to laminar complex 3D flows. Nonetheless, mild turbulence in the arteries was also rarely observed under certain circumstances. Due to this laminar and incompressible nature of the blood flows in arteries, most of the commercial CFD softwares was able to simulate reasonably accurate blood flow through arteries. Nevertheless, stationary rigid wall assumption for blood vessel in the only CFD applications is not physiologically realistic due to the fact that vessel walls are viscoelastic in nature and undergo large deformations due to hemodynamic forces, thus also affecting the blood flow dynamics passing through the vessels. According to [6] research, the rigid wall assumption in computations consistently shows an overestimation of *wall shear stress* compared to the flexible wall by as much as 50%. Consequently, accurate FSI techniques must be used while exploring the hemodynamics of blood flow in arteries. By using FSI, response of viscoelastic nature of the blood vessel into the fluid and corresponding fluid forces acting back to the vessel walls can be examined more realistically.

5.2 Blood Viscosity

Blood consists of plasma and particles, with 99% of the particle volume taken by the red blood cells, RBCs, or erythrocytes. Thus the red blood cells mainly determine the difference between plasma and blood viscosity. The viscosity of blood therefore depends on the viscosity of the plasma, in combination with the hematocrit (volume

% of red blood cells, Ht) and red cell deformability. Higher hematocrit and less deformable cells imply higher viscosity. The relation between hematocrit and viscosity is complex and many formulas exist. One of the simplest is the one by Einstein:

$$\eta = \eta_{\text{plasma}} \cdot (1 + 2.5Ht) \qquad (5.1)$$

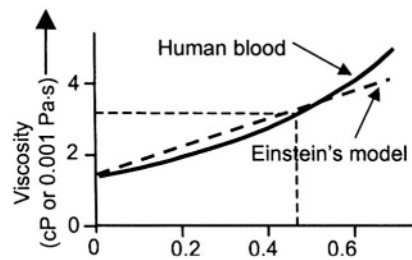Einsteins relation for the viscosity of fluids containing particles applies only to very

Figure 5.1 : Blood viscosity as function of hematocrit taken from [32]

low particle concentrations. Nevertheless, it gives some indication. The viscosity of plasma is about 0.015 Poise (1.5 centipoise, cP) and the viscosity of whole blood at a physiological hematocrit of 40 - 45% is about 3.2 cP, or $3.2 \cdot 10^{-3}$Pa.s.

Blood viscosity depends not only on plasma viscosity and hematocrit, but also on the size, shape and flexibility of the red blood cells. For instance, the hematocrit of camel blood is about half of that of human blood, but the camels red blood cells are more rigid, and the overall effect is a similar blood viscosity.

The viscosity of blood depends on its velocity. More exactly formulated, when shear rate increases viscosity decreases. At high shear rates the doughnut-shaped RBCs orient themselves in the direction of flow and viscosity is lower. For extremely low shear rates formation of RBC aggregates may occur, thereby increasing viscosity to very high values. It has even been suggested that a certain minimum shear stress is required before the blood will start to flow, the so-called yield stress. In large and medium size arteries shear rates are higher than $100s^{-1}$, so viscosity is practically constant. The physiological range of wall shear stress is 10 to 20 or 1 to 2 Pa, with 1 Pa = 0.0075 mmHg. Several equations exist that relate shear stress and shear rate of blood, e.g., Casson fluid, and Herschel-Bulkley fluid [33], [34].

Viscosity also depends on the size of blood vessel. In small blood vessels and at high velocities, blood viscosity apparently decreases with decreasing vessel size. This is known as the Fahraeus-Lindqvist effect, and it begins to play a role in vessels
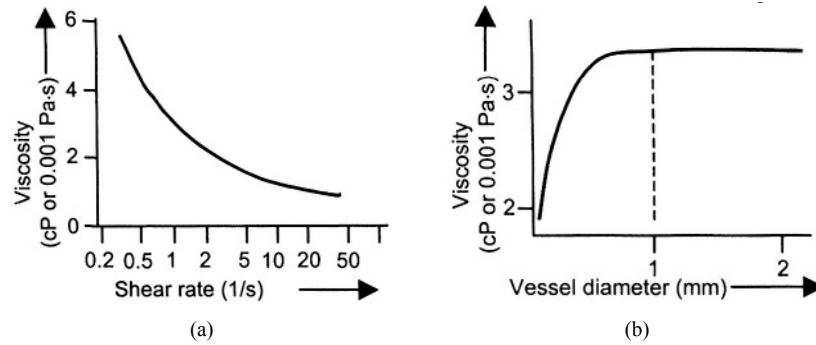
Figure 5.2 : (a)Viscosity as function of shear rate for hematocrit of 48. (b)Viscosity as function of vessel size. Taken from [32].

smaller than 1 mm in diameter. Red blood cells show axial accumulation, while the concentration of platelets appears highest at the wall. The non-Newtonian character of blood only plays a role in the microcirculation.

Viscosity depends on temperature. A decrease of $1°C$ in temperature yields a 2% increase in viscosity. Thus in a cold foot blood viscosity is much higher than in the brain.

Finally, since we simulate blood flow in large arteries, we assumed the the flow is incompressible, Newtonian and also laminar. These assumptions are good enough to be applied in our case.

5.3 Oscillatory Flow Theory and Womersley Number

The pressure-flow relation for steady blood flow, where only frictional losses are considered, and the relation between oscillatory or pulsatile pressure and flow are simplified version of the reality. However, using oscillatory or pulsatile pressure and velocity profiles in blood flow simulations gives good enough solutions for engineering purposes. That's why we also use oscillatory inlet velocity and pressure profiles in our simulations.

The relation between oscillatory, sinusoidal, pressure drop and flow through a blood vessel can be derived from the Navier-Stokes equations. The assumptions are to a large extent similar to the derivation of Poiseuilles law: uniform and straight blood vessel, rigid wall, Newtonian viscosity. The result is that flow is still laminar but pulsatile, i.e.,

37

not constant in time, and the flow profile is no longer parabolic. The theory is based on sinusoidal pressure-flow relations, and therefore called oscillatory flow theory, [35].

The flow profile depends on the frequency of oscillation, with ω the frequency, the radius r, the viscosity μ, and density ρ, of the blood. These variables were taken together in a single dimensionless parameter called Womersley number [36]. The Womersley number, or α parameter, is another dimensionless parameter that has been used in the study of fluid mechanics. This parameter represents a ratio of transient to viscous forces, just as the Reynolds number represented a ratio of inertial to viscous forces. A characteristic frequency represents the time dependence of the parameter. The Womersley number may be written as

$$\alpha = r\sqrt{\frac{\omega}{\nu}} \text{ or } \alpha = r\sqrt{\frac{\omega\rho}{\mu}} \tag{5.2}$$

where

- r = the vessel radius

- ω = the fundamental frequency

- ρ = the density of the fluid

- μ = the viscosity of the fluid

- ν = the kinematic viscosity

The fundamental frequency is typically the heart rate. The units must be rad/s for dimensional consistency. In higher-frequency flows, the flow profile is blunter near the centerline of the vessel since the inertia becomes more important than viscous forces. Near the wall, where velocity of flow, v, is close to zero, viscous forces are still important.

If the local pressure gradient, $\Delta P/l$, is a sinusoidal wave with amplitude A, and circular frequency ω, then the corresponding velocity profile is given by the formula [36]:

$$v(r,t) = Real\left(\frac{A}{\omega\rho i}\left(1 - \frac{J_0(\alpha r i^{3/2})}{J_0(\alpha R i^{3/2})}\right)e^{i\omega t}\right) \tag{5.3}$$

where α is Womersley number, A the mean velocity, r the relative radius, R the radius of the vessel, ρ the density, and ω the heart rate in rad/s.

5.4 Arterial Walls

To understand the mechanics of arterial walls, begin by imagining a long tube of constant cross section and constant wall thickness. This imaginary tube is homogeneous and isotropic (the material properties are identical in all directions). The typical blood vessel is branched and tapered. It is also nonhomogeneous and nonisotropic. Although our assumptions do not fit the blood vessel, strictly speaking, it makes a practical first estimate of a model to help understand vessel mechanics. We need to continually remember our assumptions and the limitations they bring to the model as we progress in our blood vessel simulations and modeling. Consider a
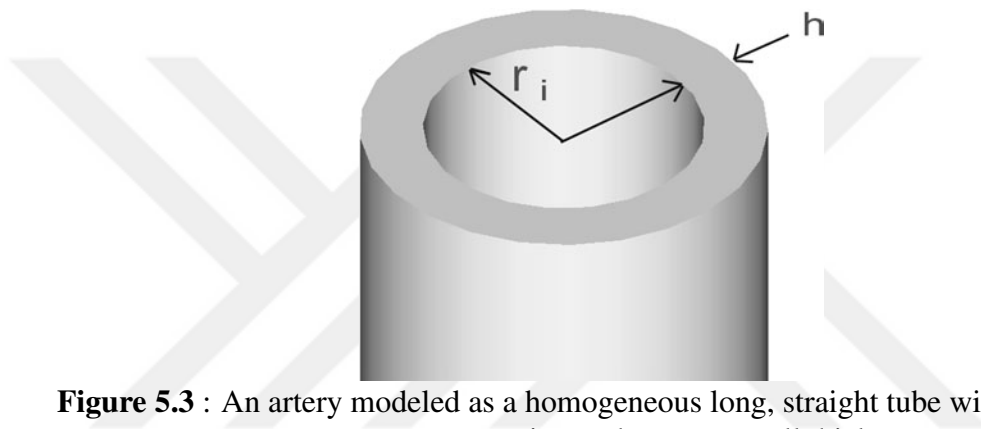

Figure 5.3 : An artery modeled as a homogeneous long, straight tube with constant cross section and constant wall thickness.

cross section of an artery as shown in Fig.5.3 with wall thickness h and inside radius r_i. Blood vessels are borderline thin-walled pressure vessels. Thin-walled pressure vessels are those with a thickness-to-radius ratio that is less than or equal to about 0.1. For arteries, the ratio of wall thickness h to inside radius r_i is typically between 0.1 and 0.15, as shown in Eq. 5.4.

$$\frac{h}{r_i} \cong 0.1 \text{ to } 0.15 \tag{5.4}$$

The mechanics of the artery are not dependent only on geometry, but rather to understand the mechanics of the artery we must also consider material properties. In order to consider material properties, lets begin with Hookes law for uniaxial loaded members. Hookes law for this simple loading condition relates stress to strain in a tensile specimen. Hookes law for a one-dimensional, uniaxial loaded member is shown in Eq. 5.5.

$$\sigma = E\varepsilon \tag{5.5}$$

where σ is the normal stress in N/m^2, E is the modulus of elasticity, N/m^2, and ε is the strain, which is unitless. For linearly elastic materials, the modulus of elasticity, E, is a constant in the linearly elastic range. However, arteries are not linearly elastic. The stressstrain curve for an artery is shown in Fig. 5.4. It is still possible to define the modulus of elasticity, but the slope of the curve varies with stress and strain. As stress increases in an artery, the material becomes stiffer and resists strain. Arteries are
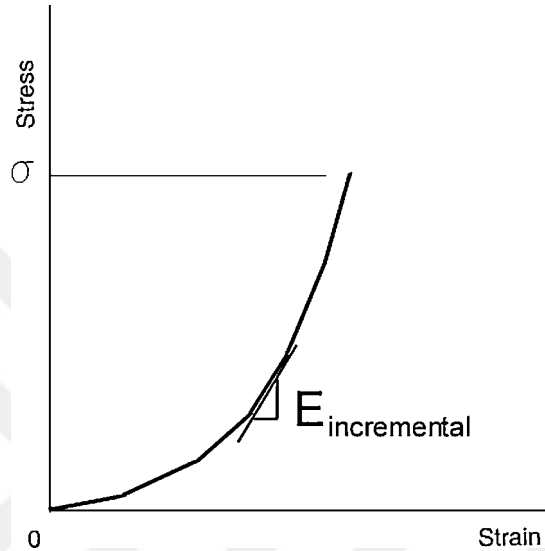

Figure 5.4 : Stress strain curve for an artery, taken from [35].

also metabolically active materials. Smooth muscle can contract and expend energy in an effort to resist strain. Also, arteries are viscoelastic materials. Viscoelasticity is a material property in which the stress is not only dependent on load and area, but also on the rate of strain. For a material in which the stress is dependent on the rate of strain, Eq. 5.6 is true.

$$\sigma = E_1\varepsilon + E_2\frac{d\varepsilon}{dt} \tag{5.6}$$

Finally, the ideal and much more realistic way to simulate blood flow through arteries with FSI, one had better use viscoelastic structure solver coupled with the flow solver. However, modeling and simulating viscoelastic structures is a challenge due to the material's nonlinear properties. In addition, coupling with a stable flow solver in a FSI application would also be a huge challenge, because the response of the structure part on the interface would have also be nonlinear which would push the limits of coupling algorithms in FSI simulations. Consequently, in order to reduce complexity of such

case, we used linear elastic model in our blood flow simulation. Nevertheless, we are fully aware of the limitations of this approach.

5.5 Blood Flow through 3D Cylinder Shaped Large Artery

In this section, we finally describe the setup parameters and also analyzing the results of our blood flow through large artery simulation ran with partitioned FSI solver.

In our simulations, we picked IQN-LS implicit partitioned coupling scheme in our FSI solver because of its being the state of the art algorithm and also it had better chance for maintaining the stability of the simulation. As discussed in the previous chapters, our problem is 3D fully enclosed incompressible FSI problem which has its own challenges, therefore by choosing IQN-LS algorithm in our FSI solver, we both obtained its performance in hemodynamics problems and also decreased the simulation's runtime lengths.

The geometry of the simulation was chosen as 3D fully enclosed. The radius of a large artery was chosen as 5mm which is consistent with the literature and reality. In order to find appropriate artery vessel wall thickness, we used equation 5.4 and decided to take the artery wall thickness as 0.75mm. The artery length was picked as 5cm which is ten times longer than the radius of the artery. This ten times length of the radius has been used for CFD application when the problem is a flow thorough a channel or a tube in order to let the flow be fully developed. The geometry of our simulation is given in figure 5.5 where, Ω_f is the flow domain, Ω_s refers to the solid domain and $\Gamma_{f,s}$ is the interface.

As can be seen from the figure 5.5, we took advantage of the axial symmetry by using the symmetry planes on both directions. Thanks to using pulsatile Womersley inlet profile which is axisymmetric. Using symmetry planes in our case reduced the computational complexity, thus simulation times significantly. In addition, we found the lowest number of mesh sizes which would have still given accurate results to further minimizing the simulation times.

The mesh properties in this case setup was given in table 5.1. As can be seen from the table, the discretization was relatively small for a case like this. There were around 23000 cells combined from both fluid and solid domains, and all of the cells were
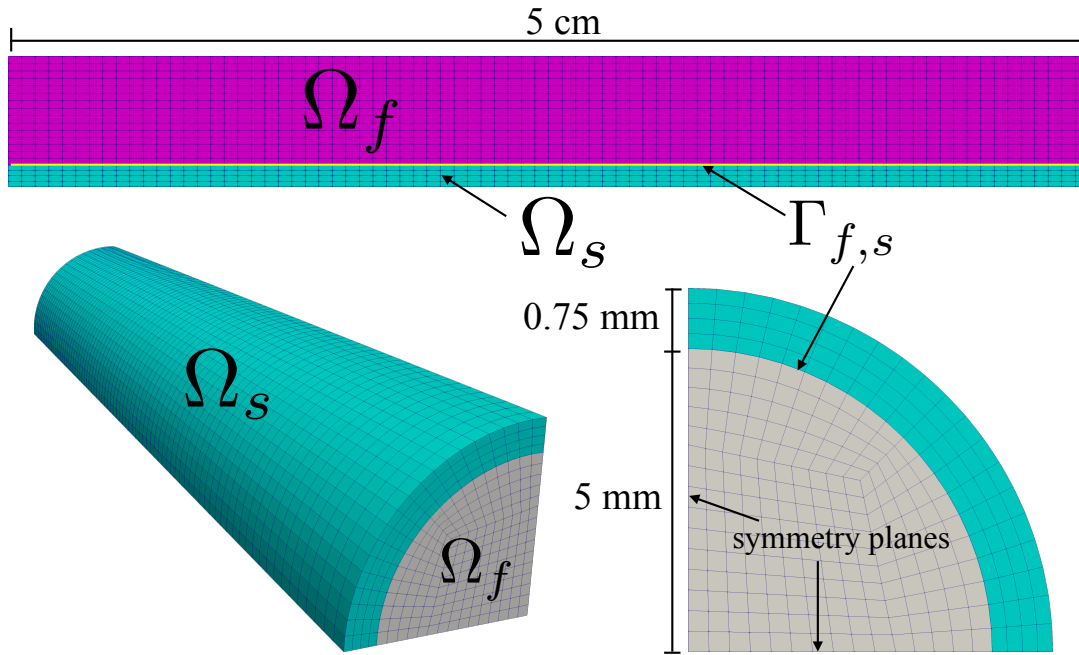
Figure 5.5 : Large artery geometry, mesh and its properties

made of hexahedra elements which are known to be good for convergence in FVM simulations.

In order to maximize numerical accuracy, stability and convergence rate of this FSI simulation, very high quality meshing was done as can be seen from the table 5.1 and the quality of the meshes were confirmed with very good maximum aspect ratio and maximum skewness measures.

In FSI simulations, conforming meshing at the coupling interface is a good practice and we applied this in our meshes too. As can be confirmed from the figure 5.5, at the coupling interface, $\Gamma_{f,s}$, the cells on the boundaries of both fluid and solid domains are conforming to each other. Therefore, we minimized the numerical errors which would have derived from the interpolations between nonconforming meshes.

Table 5.1 : 3D Large Artery Blood flow mesh properties

Stats/domain	Fluid Mesh	Solid Mesh
points	18306	8505
faces	50200	21200
cells	16000	6400
boundary patches	5	6
hexahedra elements	16000	6400
Max aspect ratio	4.63716	2.94347
Max skewness	0.726027	0.0653977

In this simulation, flow solver was chosen as incompressible, Newtonian and laminar as the reasons of this decision was explained and discussed in section 5.2. The structure solver was chosen as linear elastic as discussed in section 5.4. The transport properties of flow solver and the rheology properties of the structure solver is given in table 5.2.

Table 5.2 : Transport and rheology properties of the simulation

Properties/domain	Flow	Solid
density, ρ, kg/m^3	1060	1160
kinematic viscosity, ν, m^2/s	3e-6	-
elastic modulus, E, $kg/m \cdot s^2$	-	2e5

The inlet velocity profile was oscillatory in order to make our simulation more realistic. The velocity profile was calculated by using Womersley solution described in section 5.3. We picked the heart rate as 120 bpm which means that the frequency of the oscillatory flow would be 2 Hz. By inserting the appropriate simulation parameters into the equation 5.2, we calculated the Womersley number as:

$$\alpha = 0.01m \sqrt{\frac{120\left(\frac{\pi}{30}\right) rad/s}{3 \cdot 10^{-6} m^2/s}} = 20.467 \qquad (5.7)$$

As can be seen from the calculation of Womersley number in equation 5.7, the Womersley number in our simulation was around 20. In other words, inertial forces on the flow dominated and created a flat velocity profile. This expected flat velocity profile was showed from the results of the simulation as in figure 5.6. Due to the mesh resolutions, the velocity profile shown in the figure 5.6 is slightly different than the analytical solution of the velocity profile equation 5.3.

In figure 5.7, pulsatile blood flow and the velocity changes can be observed. Nevertheless, displacement vectors applied on the solid domain was showed in figure 5.8. As can be seen from there, the displacement vectors in front of the pulse (the reddish part of the figure) are outward, in other words, the pressure derived from the upcoming pulse have the artery walls expanded. On the other hand, the displacement vectors behind the pulse is inwards so that the artery walls contracted. Although this observation was expected due to the linear elastic model of the solid solver, however in reality, the response of the artery walls differs from this result both in the rate of strain and the amount of it.
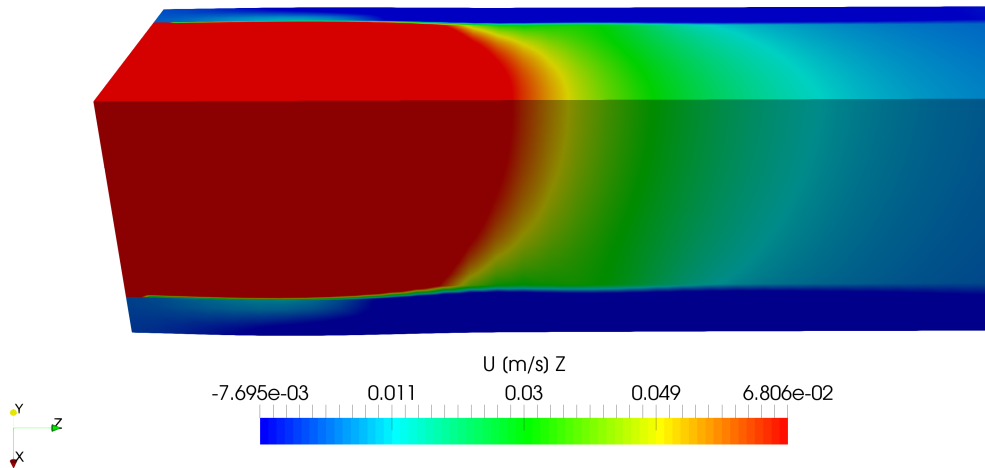
Figure 5.6 : Womersley inlet velocity profile
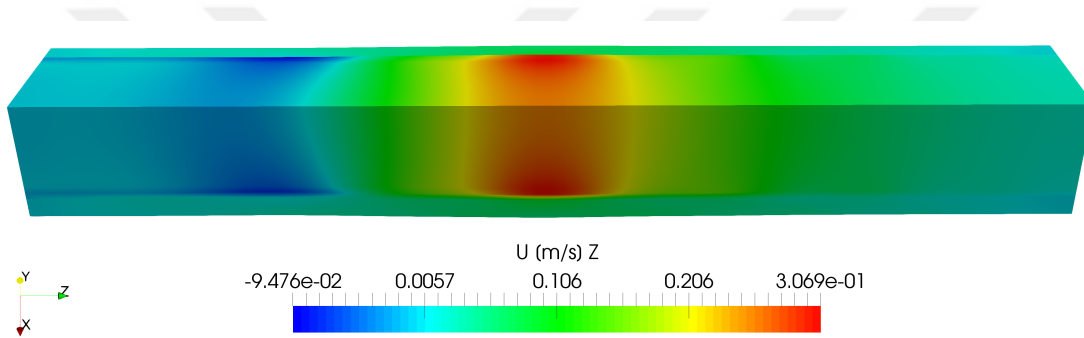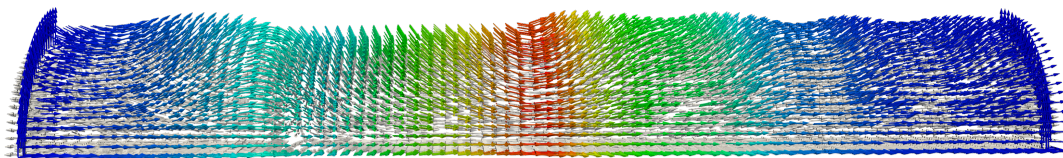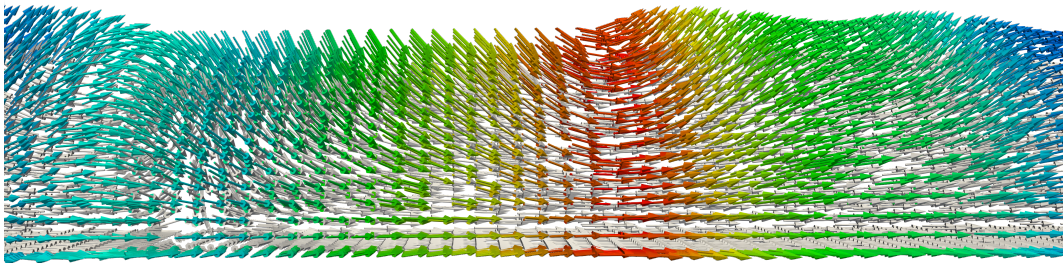

Figure 5.7 : The first pulsatile velocity passes through the middle point along the artery.
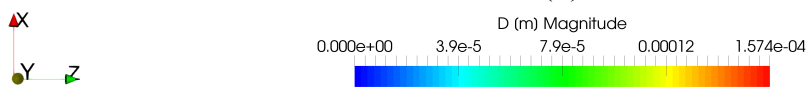

(a)

(b)

Figure 5.8 : Displacement of artery vessels during pulsatile flow passing. (a)Whole view of the problem domain. (b)Focused view of the middle part where the pulse is passing through.
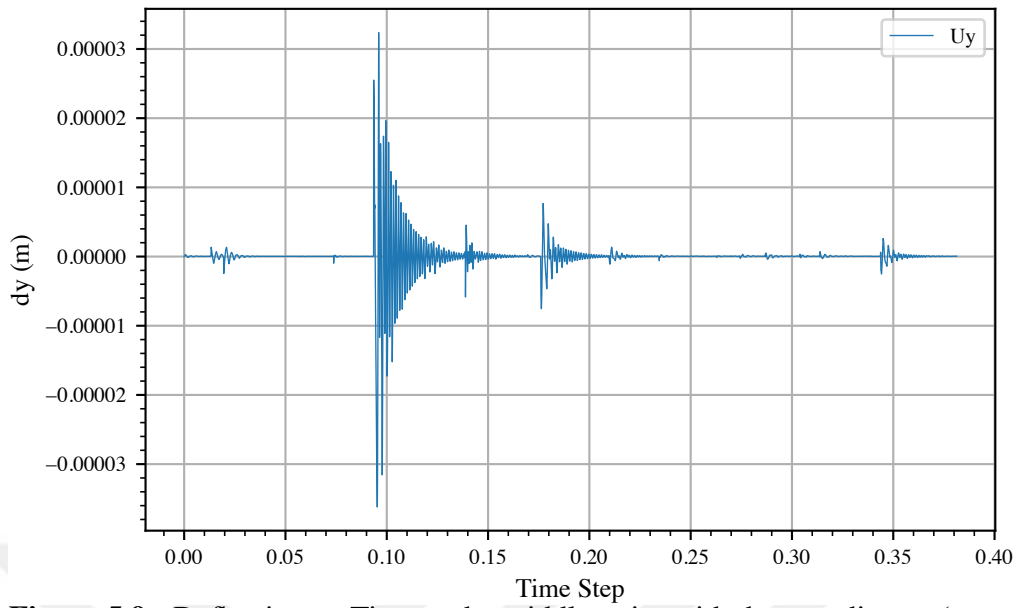
Figure 5.9 : Deflection vs Time at the middle point with the coordinates (x, y, z) = (0, 0.005, 0.025)

The deflections in time of the point with coordinates $(x, y, z) = (0, 0.005, 0.025)$ can be seen from the figure 5.9. From the graph, the expansion and the contraction of the artery walls can be read. Nonetheless, notice the effects of the first pulse and the second pulse on the displacement.
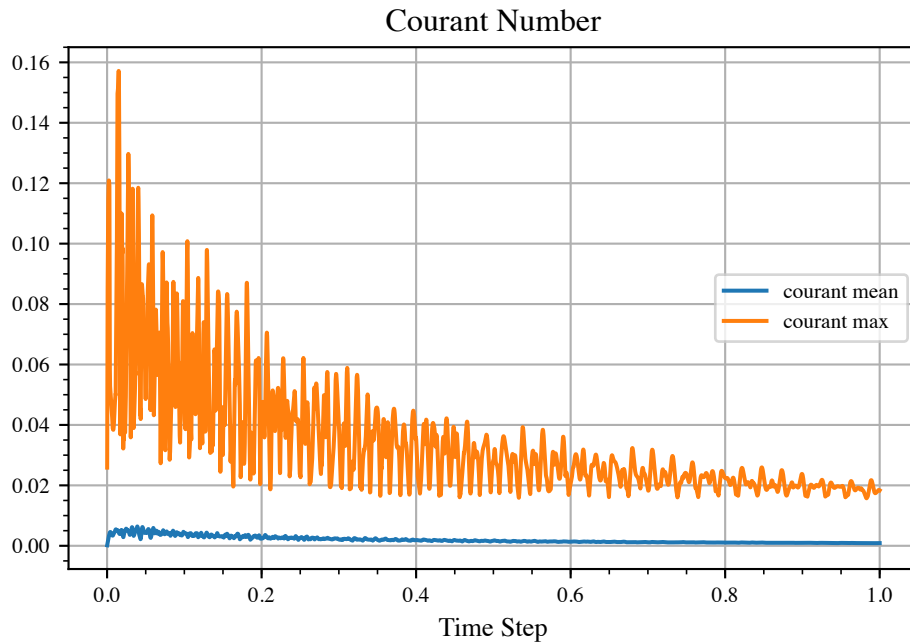

Figure 5.10 : Courant number mean and max value of fluid solver during simulation

In figure 5.10 and 5.11, the convergence and stability analysis of the simulation can be made. In CFD simulations, the Courant number and keeping it under 1 is very crucial
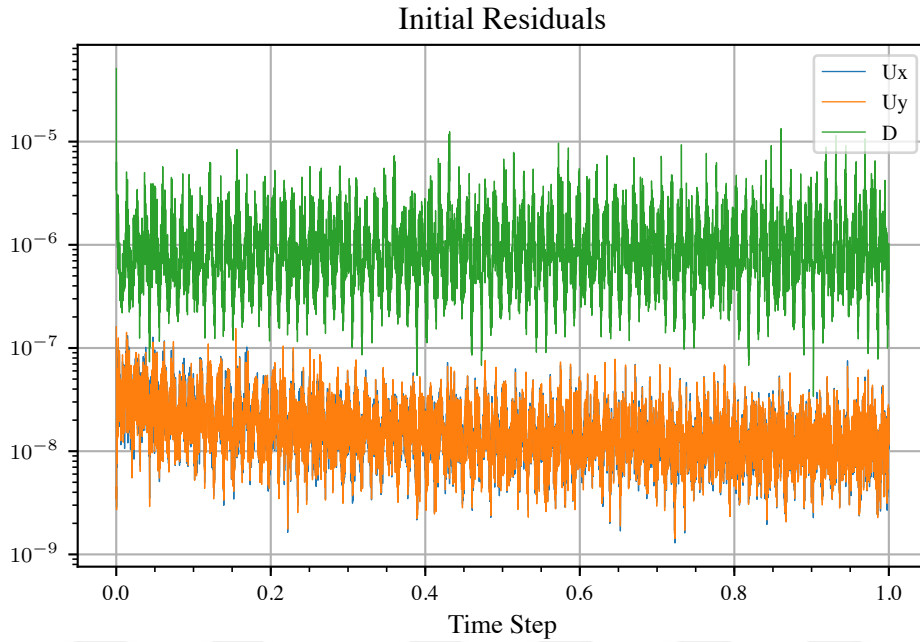
45

Figure 5.11 : Fluid solver and structural solver residuals during simulation

in order to reach convergence to the solution. Courant number gives and idea about the accuracy of the simulation. If the time step size is not selected according to the mesh sizes, then the accuracy of the solution may be compromised. Another basic check on any numerical computation is also the residuals of the unknowns. In this simulations, fluid solver solves velocities on both directions and also the structural solver solves the displacements. As can be seen from the residuals graph, initial residuals (indicates the beginning of time steps) are decreasing and they reaches to steady state with very low errors. To conclude, IQN-LS method in this case worked very well. The simulation was stable, robust and numerically accurate.

In figure 5.12, FSI coupling iterations in every time steps can be seen. Since the case geometry was 3D fully enclosed, this time number of coupling iterations started from 18 and settled on 10 to 15 band. The jump at the beginning can be explained by the nature of CFD, in other words, the beginning of a simulation is also the farthest from the converged solution and also reality. That's why, IQN-LS algorithm took more steps for convergence at the beginning time step.

5.6 Remarks

In this chapter, the essential background about hemodynamics simulation was laid out. The viscosity of blood, the mechanical properties of artery walls, the oscillatory flow
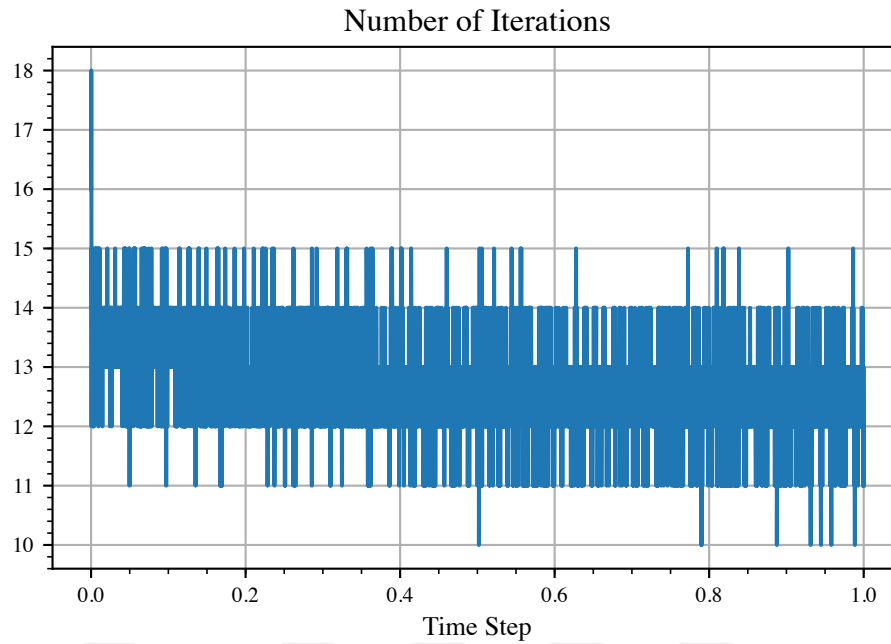
46

Number of Iterations

Figure 5.12 : Number of IQN-LS coupling iterations during simulation

theory and using Womersley number to determine the specific velocity profile were
explained briefly. Nevertheless, the state of the art FSI coupling algorithm IQN-LS
was used in order to solve blood flow through large artery in 3D. All the decisions
about the parameters of the simulation was discussed and explained.

In conclusion, IQN-LS algorithm performed very well in this blood flow simulation.
Although it was fully enclosed and incompressible flow, IQN-LS managed
convergence and stability to a solution.

6. CONCLUSIONS AND RECOMMENDATIONS

In this thesis, fluid structure interactions were explored in detail. The history of FSI applications and the motivation behind them were explained briefly. Nonetheless, different coupling algorithms in the literature were explained briefly. The differences between those algorithms were discussed both in theory and also in a benchmark case by using open source software foam-extend-3.2. In addition, artificial compressibility technique integration onto a partitioned FSI coupling algorithm, specifically onto IQN-LS, were discussed and the challenges implementing it were explained.

Fluid structure interaction in hemodynamics and in blood flow simulations were also explained. As our main focus being the blood flow simulations, we needed to have a tested, robust and flexible FSI solver. The reasons which makes using FSI techniques in blood flow simulations a necessity were discussed and examples from the literature supported those reasons.

Blood flow through large artery simulation were performed by using the state of the art FSI coupling algorithm IQN-LS and the results were analyzed in detail. Although the flow solver of the simulation and its parameters were closer to the reality, the structural solver had drawbacks as explained and discussed in detail. Nonetheless, we successfully showed that IQN-LS algorithm and foam-extend-3.2 software were suitable for blood flow simulations.

As discussed in this thesis, the advantages of using implicit partitioned FSI solvers showed great promise in our blood flow simulations. IQN-LS, being the state of the art implicit partitioned coupling algorithm, our solver can be modified in order to meet with the requirements of hemodynamics. Firstly, the linear elastic based structural can be substituted with a hyper-elastic based or viscoelastic based structural solvers depends on the problem and the targeted accuracy for the problem at hand. Secondly, for the microcirculation problems, the flow solver can be substituted with another one which models non-Newtonian flows, i.e. Bird-Carreau viscosity model. In addition, by including energy equation into the solvers and also into the IQN-LS coupling, thermal

effects can be simulated too. Those improvements can be made relatively easily and in a short amount of time thanks to the partitioned coupling scheme of the IQN-LS.

In hemodynamics, usages of patient-specific geometries and also patient-specific pressure-velocity profiles in simulations have been proved to be the most accurate results in comparison with the experimental data. However, FSI simulations with patient-specific geometries and patient-specific pressure-velocity profiles increases the complexity of those simulations significantly. However, IQN-LS in this study performed very well and as a next step, patient-specific FSI blood flow problem may be successfully solved.

Overall, we believe the work presented in this thesis to be a valuable addition to our further studies. We have built an efficient workflow on flexible, powerful, scalable and open source software for solving FSI problems which may arise in the future.

REFERENCES

[1] **Turek, S. and Hron, J.**, (2006). Proposal for numerical benchmarking of fluid-structure interaction between an elastic object and laminar incompressible flow, Fluid-structure interaction, Springer, pp.371–385.

[2] **Küttler, U., Förster, C. and Wall, W.A.** (2006). A solution for the incompressibility dilemma in partitioned fluid–structure interaction with pure Dirichlet fluid domains, *Computational Mechanics*, *38*(4), 417–429.

[3] **Farhat, C., Van der Zee, K.G. and Geuzaine, P.** (2006). Provably second-order time-accurate loosely-coupled solution algorithms for transient nonlinear computational aeroelasticity, *Computer methods in applied mechanics and engineering*, *195*(17), 1973–2001.

[4] **Piskin, S. and Celebi, M.S.** (2012). Numerical blood flow simulation with predefined artery movement, *Biomedical Engineering and Informatics (BMEI), 2012 5th International Conference on*, IEEE, pp.654–658.

[5] **Lee, C.J., Zhang, Y., Takao, H., Murayama, Y. and Qian, Y.** (2013). A fluid–structure interaction study using patient-specific ruptured and unruptured aneurysm: The effect of aneurysm morphology, hypertension and elasticity, *Journal of biomechanics*, *46*(14), 2402–2410.

[6] **Bazilevs, Y., Hsu, M.C., Benson, D., Sankaran, S. and Marsden, A.** (2009). Computational fluid–structure interaction: methods and application to a total cavopulmonary connection, *Computational Mechanics*, *45*(1), 77–89.

[7] **Tezduyar, T.E., Behr, M., Mittal, S. and Liou, J.** (1992). A new strategy for finite element computations involving moving boundaries and interfaces—the deforming-spatial-domain/space-time procedure: II. Computation of free-surface flows, two-liquid flows, and flows with drifting cylinders, *Computer methods in applied mechanics and engineering*, *94*(3), 353–371.

[8] **Bazilevs, Y., Takizawa, K. and Tezduyar, T.E.** (2013). Advanced FSI and Space–Time Techniques, *Computational Fluid-Structure Interaction: Methods and Applications*, 139–169.

[9] **Causin, P., Gerbeau, J.F. and Nobile, F.** (2005). Added-mass effect in the design of partitioned algorithms for fluid–structure problems, *Computer methods in applied mechanics and engineering*, *194*(42), 4506–4527.

[10] **Degroote, J.**, **Bathe, K.J. and Vierendeels, J.** (2009). Performance of a new partitioned procedure versus a monolithic procedure in fluid–structure interaction, *Computers & Structures*, *87*(11), 793–801.

[11] **Degroote, J.**, **Swillens, A.**, **Bruggeman, P.**, **Haelterman, R.**, **Segers, P. and Vierendeels, J.** (2010). Simulation of fluid–structure interaction with the interface artificial compressibility method, *International Journal for Numerical Methods in Biomedical Engineering*, *26*(3-4), 276–289.

[12] **Kassiotis, C.**, **Ibrahimbegovic, A.**, **Niekamp, R. and Matthies, H.G.** (2011). Nonlinear fluid–structure interaction problem. Part I: implicit partitioned algorithm, nonlinear stability proof and validation examples, *Computational Mechanics*, *47*(3), 305–323.

[13] **Badia, S.**, **Nobile, F. and Vergara, C.** (2008). Fluid–structure partitioned procedures based on Robin transmission conditions, *Journal of Computational Physics*, *227*(14), 7027–7051.

[14] **Dettmer, W.G. and Perić, D.** (2008). On the coupling between fluid flow and mesh motion in the modelling of fluid–structure interaction, *Computational Mechanics*, *43*(1), 81–90.

[15] **Vierendeels, J.**, **Lanoye, L.**, **Degroote, J. and Verdonck, P.** (2007). Implicit coupling of partitioned fluid–structure interaction problems with reduced order models, *Computers & structures*, *85*(11), 970–976.

[16] **Hirt, C.**, **Amsden, A.A. and Cook, J.** (1974). An arbitrary Lagrangian-Eulerian computing method for all flow speeds, *Journal of computational physics*, *14*(3), 227–253.

[17] **Tang, T.** (2013). Implementation of solid body stress analysis in OpenFOAM, **Technical Report**.

[18] **Bazilevs, Y.**, **Takizawa, K. and Tezduyar, T.E.** (2013). Governing Equations of Fluid and Structural Mechanics, *Computational Fluid-Structure Interaction: Methods and Applications*, 1–35.

[19] **Bazilevs, Y.**, **Takizawa, K. and Tezduyar, T.E.** (2013). ALE and Space–Time Methods for Moving Boundaries and Interfaces, *Computational Fluid-Structure Interaction: Methods and Applications*, 83–109.

[20] **Bazilevs, Y.**, **Takizawa, K. and Tezduyar, T.E.** (2013). ALE and Space–Time Methods for FSI, *Computational Fluid-Structure Interaction: Methods and Applications*, 111–137.

[21] **Kassiotis, C.** (2009). Nonlinear fluid-structure interaction: a partitioned approach and its application through component technology, *Ph.D. thesis*, Université Paris-Est.

[22] **Jasak, H.**, The OpenFOAM Extend Project (Community-driven Releases of Open-FOAM).

[23] **Jasak, H.**, **Jemcov, A.**, **Tukovic, Z.** *et al.* (2007). OpenFOAM: A C++ library for complex physics simulations, *International workshop on coupled methods in numerical dynamics*, volume1000, IUC Dubrovnik, Croatia, pp.1–20.

[24] **Tukovic, Z.**, **Cardiff, P.**, **Karac, A.**, **Jasak, H. and Ivankovic, A.** (2014). OpenFOAM library for fluid structure interaction, *9th OpenFOAM Workshop, Zagreb, Croatia*.

[25] **Förster, C.**, **Wall, W.A. and Ramm, E.** (2007). Artificial added mass instabilities in sequential staggered coupling of nonlinear structures and incompressible viscous flows, *Computer methods in applied mechanics and engineering*, *196*(7), 1278–1293.

[26] **Küttler, U. and Wall, W.A.** (2008). Fixed-point fluid–structure interaction solvers with dynamic relaxation, *Computational Mechanics*, *43*(1), 61–72.

[27] **Willcox, K. and Peraire, J.** (2002). Balanced model reduction via the proper orthogonal decomposition, *AIAA journal*, *40*(11), 2323–2330.

[28] **Degroote, J.**, **Haelterman, R.**, **Annerel, S.**, **Bruggeman, P. and Vierendeels, J.** (2010). Performance of partitioned procedures in fluid–structure interaction, *Computers & structures*, *88*(7), 446–457.

[29] **Raback, P.**, **Ruokolainen, J.**, **Lyly, M. and Järvinen, E.** (2001). Fluid-structure interaction boundary conditions by artificial compressibility, *ECCOMAS Computational Fluid Dynamics Conference, Swansea, UK*.

[30] **Riemslagh, K.**, **Vierendeels, J. and Dick, E.** (2000). An efficient coupling procedure for flexible wall fluid-structure interaction, *3th European Congress on computational methods in applied sciences and engineering, Barcelona, Spain*, volume 13.

[31] **Bogaers, A.E.J.** (2015). Efficient and robust partitioned solution schemes for fluid-structure interactions, *Ph.D. thesis*, University of Cape Town.

[32] **Waite, L. and Fine, J.M.** (2007). Applied biofluid mechanics.

[33] **Errill, E.** (1969). Rheology of blood, *Physiological reviews*, *49*(4), 863–888.

[34] **Scott Blair, G.W.**, **Spanner, D.C.** *et al.* (1974). *Introduction to biorheology*, Elsevier Scientific Publ. Co.

[35] **Westerhof, N.**, **Stergiopulos, N. and Noble, M.I.** (2010). *Snapshots of hemodynamics: an aid for clinical research and graduate education*, Springer Science & Business Media.

[36] **Womersley, J.** The mathematical analysis of the arterial circulation in a state of oscillatory motion. 1957, Wright Air Dev, **Technical Report**, Center, Tech Report WADC-TR-56-614.
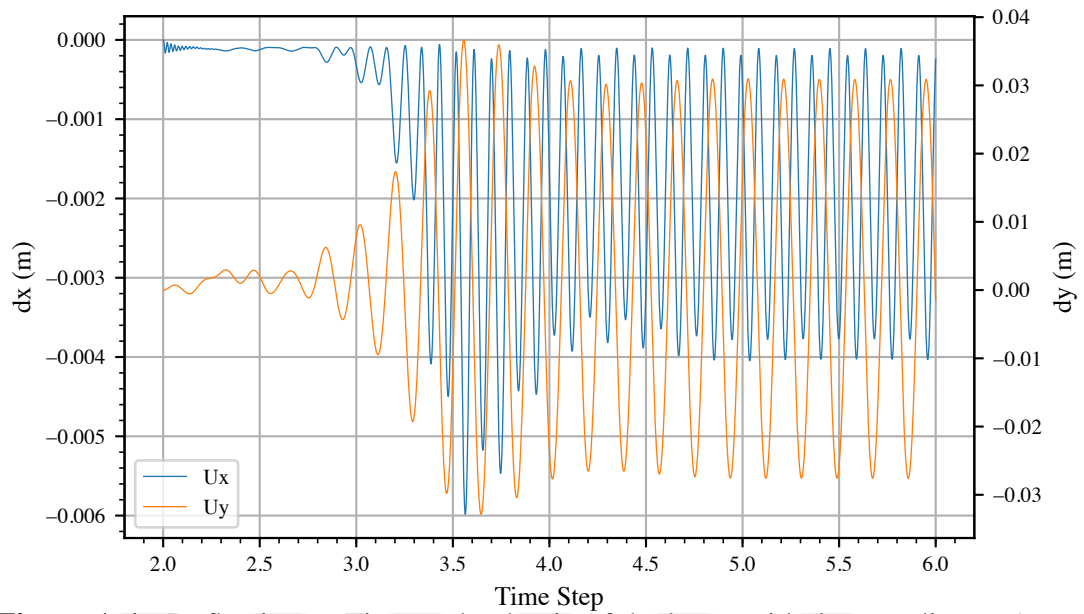
APPENDICES

APPENDIX A.1 : Benchmark Case Results

Figure A.1 : Deflection vs Time at the the tip of the beam with the coordinates (x, y, z) = (0.6 0.2 0.025334) during simulation with Aitken's relaxation method
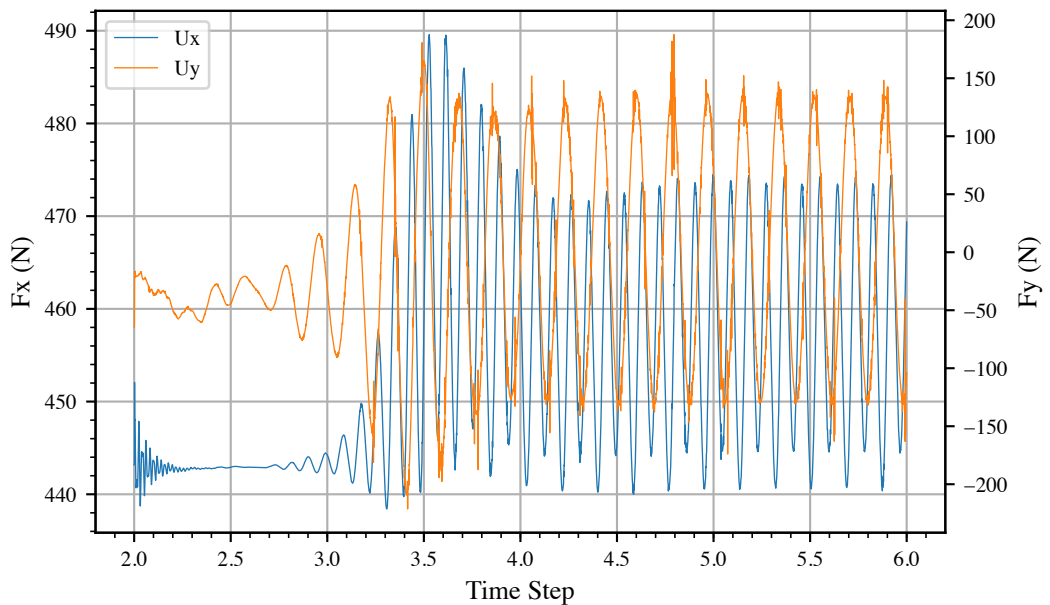

Figure A.2 : Forces vs Time at the the tip of the beam with the coordinates (x, y, z) = (0.6 0.2 0.025334) during simulation with Aitken's relaxation method
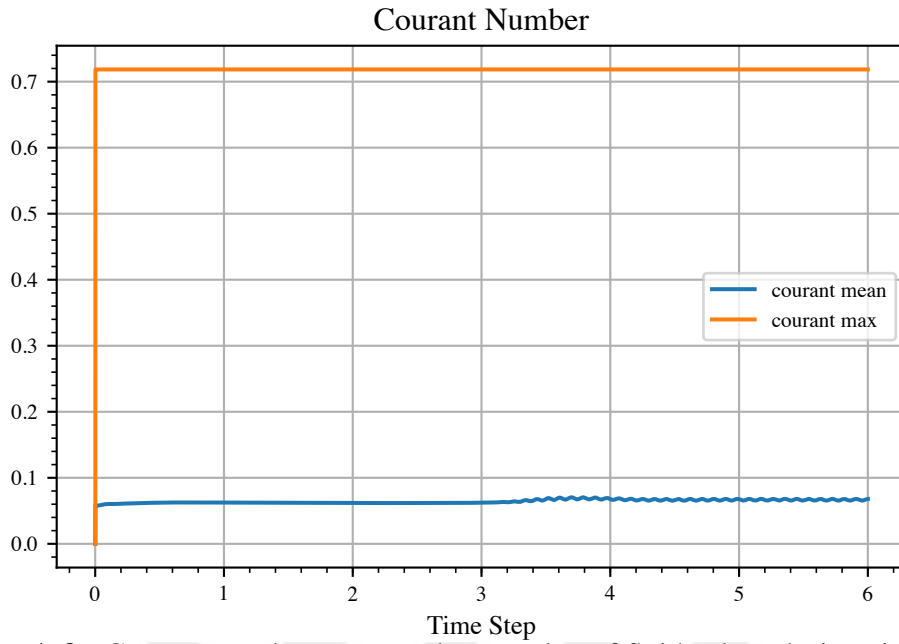
Figure A.3 : Courant number mean and max value of fluid solver during simulation with Aitken's relaxation method
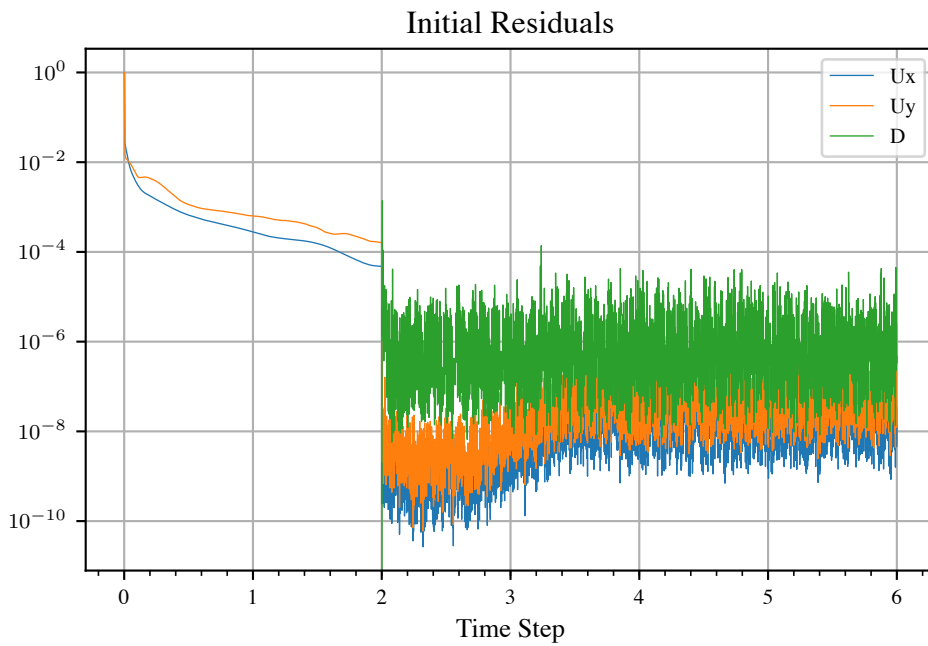

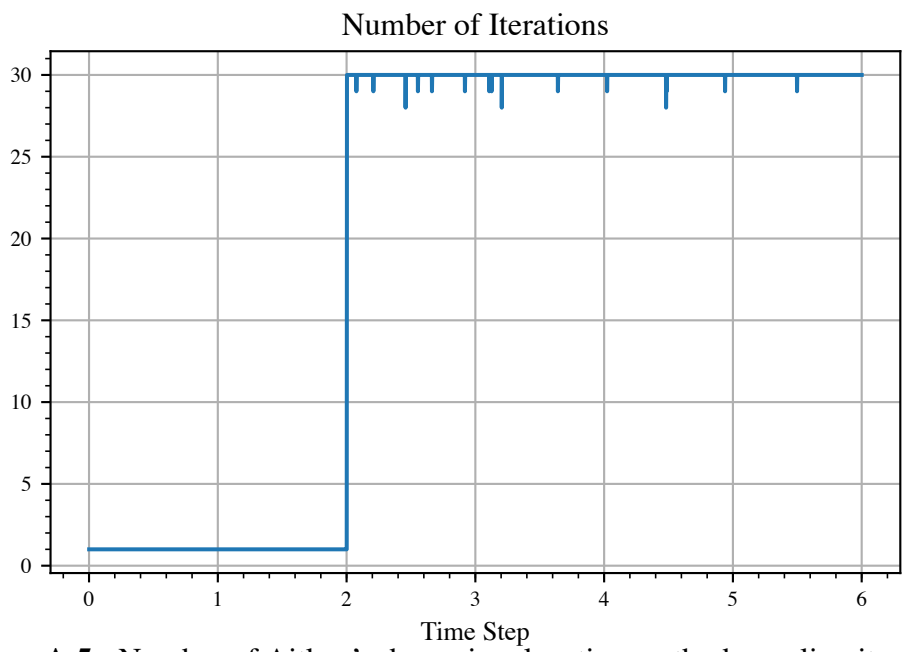**Figure A.4** : Fluid solver and structural solver residuals during simulation with Aitken's relaxation method

Figure A.5 : Number of Aitken's dynamic relaxation method coupling iterations during simulation

CURRICULUM VITAE

Name Surname: İbrahim Özküçük

Place and Date of Birth: İstanbul, 1987

E-Mail: iozkucuk@itu.edu.tr

EDUCATION:

- **M.Sc.:** 2017, Istanbul Technical University, Computational Science and Engineering
- **B.Sc.:** 2011, Sabancı University, Mechatronics Engineering

PROFESSIONAL EXPERIENCE AND REWARDS:

- Concept Design Engineer: 2011, Repkon Machine and Tool Industry and Trade Inc.

PUBLICATIONS, PRESENTATIONS AND PATENTS ON THE THESIS: